



Identification of a monitoring nonlinear oil damper using particle filtering approach

Yunjia Tong^a, Liyu Xie^a, Songtao Xue^{a,b}, Hesheng Tang^a

^a Dept. of Disaster Mitigation for Structures, Tongji University, Shanghai 200092, China

^b Dept. of Architecture, Tohoku Institute of Technology, Sendai 982-8577, Japan

ARTICLE INFO

Communicated by Eleni Chatzi

Keywords:

Damper identification
Nonlinear viscous damper
Fluid viscous damper
Maxwell model
Kelvin-Voight model
Particle filtering
Parameter identification

ABSTRACT

Oil dampers have been used in recent years for passive structural control and shock mitigation in dynamic structural systems. However, machining technical and economic problems limit its application for new and existing buildings due to the necessary precision machining of incorporating shaft bearings and pressure sealings. A kind of nonlinear oil damper that is quite different from traditional oil damper is investigated and applied to a steel building. Vibration monitoring system was instrumented on the dampers to explore their actual performance and effectivity under strong earthquakes. Based on monitoring response of the nonlinear dampers under various excitations, Bayesian model selection is employed to analyze the most probable model class which can capture main dynamic characteristics of the nonlinear oil dampers and can also be used for predicting future response as well as reliability. Then, a particle filtering approach is proposed to identify the nonlinear model of the damper and quantify the model uncertainty. The developed particle filter is capable of re-parameterizing joint posterior distribution of states and parameters of the nonlinear oil damper without augmented state estimation, which combined with Markov chain Monte Carlo algorithm so as to be able to sample high-dimensional posterior distribution. The identified models and posterior distributions of parameters show that the developed particle filter approach can be appropriately used for nonlinear parameter identification without stuck to special particles. Furthermore, the dynamic properties of the nonlinear oil damper with respect to various excitations involving different spectral characteristics are discussed.

1. Introduction

Vibration reduction has been a major concern in civil engineering for many years as a result of earthquake, wind, etc., especially in earthquake-prone area [1]. When an earthquake strikes structures, the earthquake incurs substantial energy to structures, the structures then transform part of input energy into kinetic energy, deposit part of input energy in elastic deformations as potential energy, and dissipate the remaining through inherent damping. Whenever the potential energy demand exceeds capacity of elastic deformations, the structural element yields and even damages. Thus, special designed protective systems are proposed to protect the structures.

The protective systems either isolate the structures out of reaching of input energy or dissipate or absorb the energy by themselves [2]. Base isolator is designed to separate the structures from most of energy through filtering them out. On the other hand, energy absorber devices are proposed to extract energy from the structures. Among all kinds of energy dissipation systems, fluid viscous dampers have long been attractive for new and existing buildings in vibration control [3].

Fluid viscous dampers originated from buffers of overhead crane in early 1960's, and were used extensively as shock isolator for

<https://doi.org/10.1016/j.ymssp.2022.110020>

Received 2 June 2022; Received in revised form 31 October 2022; Accepted 5 December 2022

Available online 28 December 2022

0888-3270/© 2022 Elsevier Ltd. All rights reserved.

aerospace and military industry [4,5]. It was not until late 1980s that fluid viscous dampers were introduced to civil engineering. In 1985, seismic isolation of building in terms of earthquake protection and vibration control was developed [6]. In 1990s, Makris and Constantinou [5,7-12] tested and modeled a cylindrical damper whose piston had the ability of all directions motion, and produced damping forces through the motion. Hereafter, all kinds of fluid viscous dampers with different geometry were proposed and studied [13-20].

The fluid viscous dampers are typically made up of a piston and a cylinder, while the piston separates the cylinder into two compartments, with which are immersed highly viscous liquid [21]. Therefore, the property of the viscous liquid directly determines the fluid viscous damper's dynamic characteristics and hence energy absorbing effectivity. Viscous oil dampers (hereinafter referred to as oil dampers) are recently often adopted for new-built and retrofitted buildings, as oil dampers are almost temperature independent and possess stable mechanical properties [22,23]. Moreover, oil dampers are relatively low frequency dependency comparing to strongly frequency dependency of general viscous dampers.

Research works have been done on investigating dynamic behavior and mathematical model of oil dampers [2,24-27]. As a kind of additional passive damping devices, oil dampers have been well-established and used extensively in new and retrofit constructions in recent years. Nevertheless, the oil dampers are relatively expensive due to the necessary precision machining of incorporating shaft bearings and pressure sealings. For the purpose of addressing this challenge, a novel oil damper is proposed with a gap between cylinder and piston, packing with viscoelastic polymer, which make soft rings to allow relative motion between the pistons and cylinder, and to serve to seal pressurized fluid. Thus, the novel oil damper enables easy production and less costly [28].

The mathematical model for oil damper has been considered as a linear viscous dashpot, therefore, the hysteretic behavior of oil damper brace can be represented by a Maxwell model with a spring connected in series with a dashpot [2,10,25,27,29,30]. Nevertheless, the novel oil damper also produces viscoelastic resisting force by shear motion of sealing rings except the resisting force from inner pressure differential of fluid when oil flows through orifice. Therefore, analytical model for the novel oil damper brace incorporating the bracing frame is complicated and nonlinear. At the same time, the mathematical model for the novel oil damper brace is crucial to be incorporated into structural computational models, and for successful application in design practice, as well as for model updating and prediction using vibration data in structural health monitoring. Studies have been done to investigate the dynamic behaviors of the novel oil dampers experimentally in small-scale implementations [28,31], which explicitly focus on the implementation of the novel oil dampers to mitigate seismic vibration of structures. With the progress of the novel oil dampers from theoretical designs into practical applications, reliable methods for model identification are necessary to assess if the damper is working as designed and validate the expected performance.

Various nonlinear identification methods are being developed for accurately identification of such nonlinear devices, e.g. black-box model identifications [32,33], restoring force methods [34], artificial neural networks strategies [35-38], as well as differential evolution approaches [39]. Bayesian techniques offer a prospective alternative other than above methods, which have been used recently and proven to be useful for model selection and parameter estimation in nonlinear systems. Among Bayesian techniques, two sorts of filter algorithms, that is, the Kalman filter and particle filter are able to recursively and almost real-time estimate highly nonlinear systems from noisy data. Kalman filter family series include linear optimal estimation algorithm (Kalman filter itself) and nonlinear filters such as the unscented Kalman filter (UKF) and extended Kalman filter (EKF) [31], which all have a prerequisite of Gaussian assumption. While particle filter algorithm is capable of coping with non-Gaussian or unknown distribution, which estimates the posterior density distribution merely using a group of random samples from that density. The particle filter series algorithms have been studied numerically and shown to be robust to noise regardless of degree of nonlinearity [40].

In this study, the novel oil dampers are applied to an eight-story passively-controlled steel building serving as passive energy absorber. In order to investigate actual performance and dynamic characteristics of the new type oil dampers, vibration monitoring system was instrumented on the dampers. Based on monitoring response of the nonlinear dampers under various excitations, Bayesian model selection is employed to pick the most probable model class which captures the main dynamic characteristics of the new type oil dampers and can also be used for predicting future response as well as reliability. To further probe the hysteretic behavior and damping characteristics of the nonlinear oil damper with respect to various earthquake excitations, analytical models of the nonlinear oil dampers are identified with model uncertainties quantified by improved particle filter algorithm. The developed particle filter is capable of re-parameterizing joint posterior distribution of states and parameters of the nonlinear oil damper without augmented state estimation, which combined with Markov chain Monte Carlo algorithm so as to be able to sample high-dimensional posterior distribution. The identified models and posterior distributions of parameters show that the developed particle filter approach can be appropriately used for nonlinear parameter identification without stuck to special particles. Furthermore, the dynamic properties of the nonlinear oil damper with respect to various excitations involving different spectral characteristics are discussed.

2. Viscous oil dampers

Fluid viscous dampers (FVDs) have been developed and used as supplemental damping devices in structural systems in order to suppress structural vibrations incurred by earthquake or wind loads. Various viscous dampers have been investigated both experimentally and analytically, and shown to be capable of effectively dissipating input energy from structural systems, thereby reducing seismic response of structural and non-structural systems. Among various viscous dampers, viscous oil damper is advantageous as the oil damper can produce high damping force and is also attractive to be designed in compact form for new or retrofitted buildings. What's moreover, oil damper is almost temperature independent and possesses stable mechanical properties in comparison with solid viscoelastic dampers, which is relatively high temperature dependent.

2.1. Hysteretic behavior of generalized viscous oil dampers

In general, oil dampers are typically made up of circular plates with orifices and a container, within which the circular plates are placed on top. The circular plates with orifices are usually referred to as piston head, and compartment between the piston head and container is full of highly viscous fluid, e.g. silicone oil or a type of similar oil. The damper force is then developed from inner pressure differential resistance, when the viscous oil flows through an orifice. Relationship of the damper force and velocity is dictated by designed dimension of the orifice. a common practice for viscous dampers has been to ignore the axial stiffness of dampers as it's usually very small, and the viscous dampers are then assumed to be purely viscous dashpot model. Consequently, the generalized relationship of the damper force and velocity of the general oil dampers can be expressed in mathematical form as follows:

$$f_d(t) = \text{sgn}(\dot{x}_d(t))c_d|\dot{x}_d(t)|^\alpha \tag{1}$$

in which, $f_d(t)$ is axial force of the oil dampers, $\text{sgn}(\cdot)$ is signum function, $x_d(t)$ and $\dot{x}_d(t)$ are displacement and velocity of the oil dampers, c_d denotes the viscous damping coefficient, α represents the velocity exponent which is dictated by the property of the viscous liquid and designed dimension of the orifice.

To further investigate the hysteretic behavior of generalized viscous oil dampers, a harmonic excitation is enforced to simulate dynamic behavior of the oil dampers, which can be described as $x_d(t) = x_{d,max}\sin(\omega t)$. Thus, the maximum damper force can then be expressed as follows:

$$f_{d,max} = c_d(\omega x_{d,max})^\alpha \tag{2}$$

where $x_{d,max}$ and $f_{d,max}$ represent amplitude of the peak displacement and damper force, respectively. ω denotes the circular frequency of the harmonic sinusoidal excitation. Thus, the relationship curves of the normalized damper force versus velocity or displacement of the generalized viscous oil dampers are shown as in Fig. 1 when the velocity exponent α varies [41].

As can be observed from Fig. 1, for $\alpha = 1$, the damper force versus velocity relation of viscous damper becomes linear, and the damper force versus displacement hysteretic loop turns into a circle. While hysteresis loop of the damper force versus displacement turns into rectangular for $\alpha = 0$, which is the typical analytical models of friction dampers [42]. For $\alpha > 1$, the viscous dampers produce larger forces with higher velocity, and are usually utilized to absorb shock wave which happens in a moment. Noteworthy that such dampers may generate excessive interaction forces to immediately adjacent structure systems, which is obviously undesirable for seismic vibration control of buildings. Therefore, $\alpha \leq 1$ is most often chose for seismic design applications. As a result, linear oil dampers have been extensively applied in recent years for passive structural control and shock mitigation in dynamic structural systems. In order to prevent excessive damper forces from occurring for special case in applications, e.g. intense ground motion strikes, a relief mechanism is usually introduced to those oil dampers. If the relief force the oil dampers is reached, the damping coefficient turns small, thus, the maximum damper force of the oil dampers could be within a reasonable range.

2.2. Characteristics of novel nonlinear oil dampers

Oil dampers are usually utilized for inter-story installation to enhance the structural performance, as they can slash both the deformation and force demand of the structures. Therefore, viscous oil dampers have been especially attractive as a kind of typical energy dissipation devices. Nevertheless, the oil dampers are relatively expensive due to the necessary precision machining of

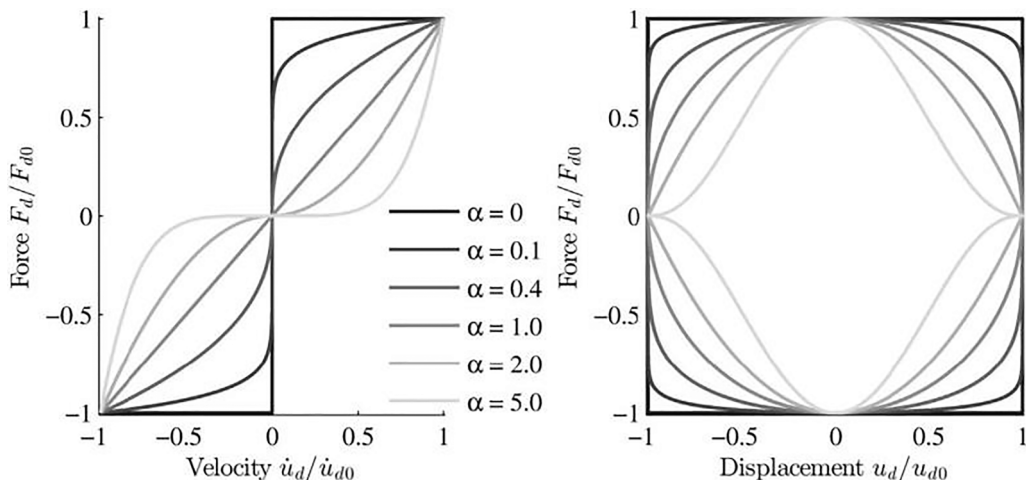


Fig. 1. Relation curves of the normalized damper force versus velocity.

incorporating shaft bearings and pressure sealings. For the purpose of addressing this challenge, a novel oil damper is proposed with a gap between cylinder and piston, packing with viscoelastic polymer, which make soft rings to allow relative motion between the pistons and cylinder, and to serve to seal pressurized fluid. Thus, the novel oil damper enables easy production and less cost [28]. Moreover, the improved nonlinear oil damper is capable of obtaining similar effectivity of vibration control with a much smaller damper force.

Scheme of the proposed nonlinear oil damper is illustrated in Fig. 2. The oil damper consists of two pistons and a cylinder, and the pair of pistons are integrated together through outer framework so as to move together. A diaphragm partitions the cylinder into two compartments, which are filled with viscous oil. A bolt is then put through the above diaphragm and bored an axial hole of a small diameter, thus, an orifice for oil flow is formed. A special construct of the oil damper is proposed that the gap between pistons and cylinder is packed with viscoelastic polymer, which make soft rings to allow relative motion between the pistons and cylinder, and to serve to seal pressurized fluid. Whenever displacement is enforced on the pistons, the soft rings of viscoelastic polymer experience dynamic shear deformation, and the contained viscous oil flows through the narrow orifice simultaneously. Thus, resisting forces stemmed from viscoelastic shear deformation and inner pressure differential of fluid are produced by the novel oil damper.

The nonlinear oil dampers are then applied to an eight-story passively-controlled steel building, which is the Administration Building on the main campus of the Tohoku Institute of Technology located in Sendai. The building's main structural system is braced steel frames, which is 48m long, 9.6m wide, and 34.2m high with 3 bays in transverse direction and 10 bays in longitudinal direction, as illustrated in Fig. 3. The building was designed in line with Japanese Earthquake Resistance Code for School Buildings. In order to testify the effectivity of the novel developed nonlinear oil dampers and enhance seismic resistance capability of the building, 56 sets of dampers were installed in the building with total eight sets of oil dampers on each floor, four sets of oil dampers in each direction. Detailed allocation of oil dampers can be seen in Fig. 3. The oil dampers are implemented through the V-type steel braces between the adjacent floors, as depicted in Fig. 3 and Fig. 4. Two kinds of nonlinear oil dampers with different orifice specifications and stroke limits of relief mechanism are utilized for 1st floor (Type I) and 3rd to 8th floor (Type II), respectively. The first two floors are merged to constitute a large space with a height of 8 m [43].

In order to further investigate actual performance and dynamic characteristics of the new type of oil dampers, vibration monitoring system was instrumented on the dampers. Displacement-meters were mounted on the dampers to measure the relative story displacement, and strain gauges were also deployed to measure axial forces of the oil damper braces. The distribution of load cell gauge and displacement transducers on the oil damper is depicted as in Fig. 5. Since all kinds of sensors were instrumented on the dampers on 2003, the vibration monitoring system has accumulated large amount of valuable data. Among them, the recorded earthquakes with magnitude greater than 7 were employed to train and predict the model response of the nonlinear oil damper braces. Table 1 lists the detail specifications of the recorded earthquakes in terms of their time, date, location, depth, epicentral distance as well as magnitude. What's more, the recorded data about damper force, displacement and hysteretic behavior for oil dampers (Type II) in longitude direction are also displayed in Fig. 6, which will be used for further analysis.

3. Models selection for monitoring nonlinear oil dampers

3.1. Analytical model for novel nonlinear oil dampers

The novel oil dampers compose of a cylinder and a pair of pistons and are connected through the V-type steel braces between the adjacent floors. The pair of pistons are installed in the U-type abutment which is fixed on the floor, while the central cylinder is mounted onto the V-type brace, as shown in as in Fig. 7. Thus, the central cylinder moves relative to the pistons back and forth in horizontal direction. Take an assumption that the stiffness of the rigid V-type braces is infinite and the corresponding deformation is negligible, consequently, the displacement of oil damper brace equals to the inter-story drift. The dimension of the novel oil damper is 424 mm wide and 328 mm high, moreover, two types of nonlinear oil dampers with different orifice specifications and stroke limits of relief mechanism are utilized for 1st floor (Type I) and 3rd to 8th floor (Type II), respectively. Detail construction of the novel oil

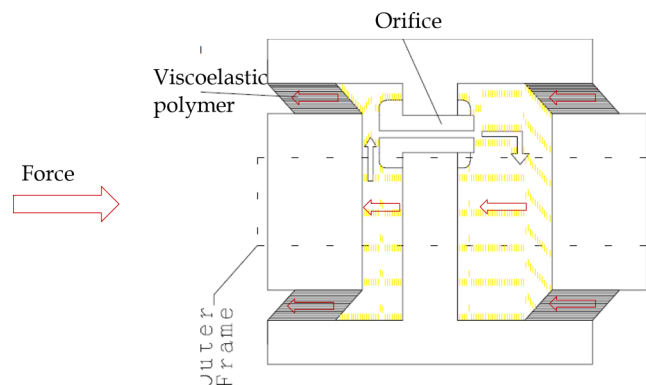


Fig. 2. Scheme of the proposed nonlinear oil damper.

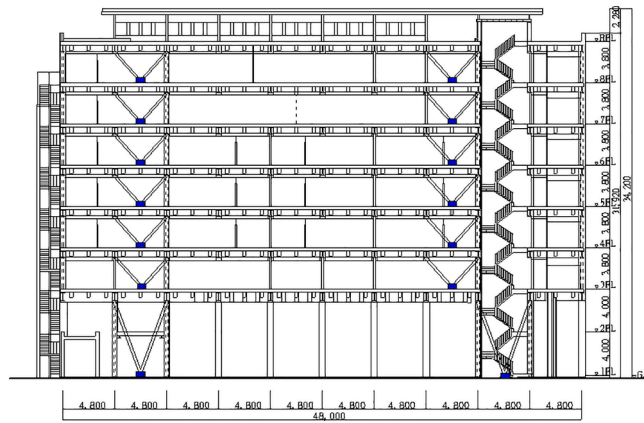


Fig. 3. Allocation of oil dampers.



Fig. 4. Oil damper brace.

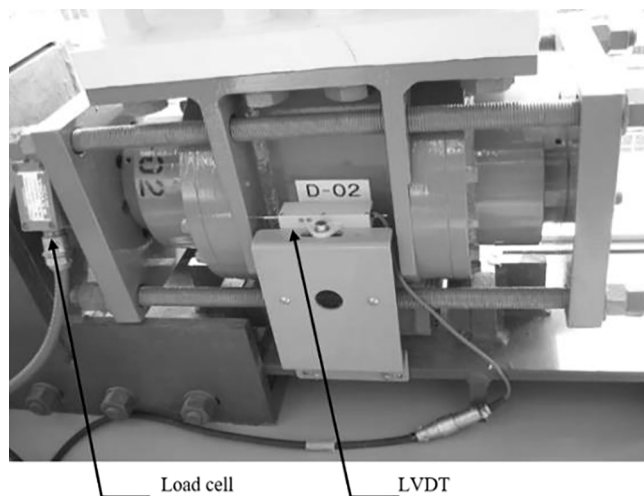


Fig. 5. Detail position of sensors distribution.

Table 1
Information of earthquakes.

Date	Time	Location		Epicentral distance	Depth	Magnitude
(y/m/d)	(UTC)	N (°)	E (°)	(km)	(km)	M
2003/5/26	9:24:33	38.849	141.568	88.6	68	7
2005/8/16	2:46:28	38.276	142.039	102.1	36	7.2
2011/3/9	2:45:20	38.435	142.842	173	32	7.3
2011/4/7	14:32:43	38.276	141.588	62.7	42	7.1

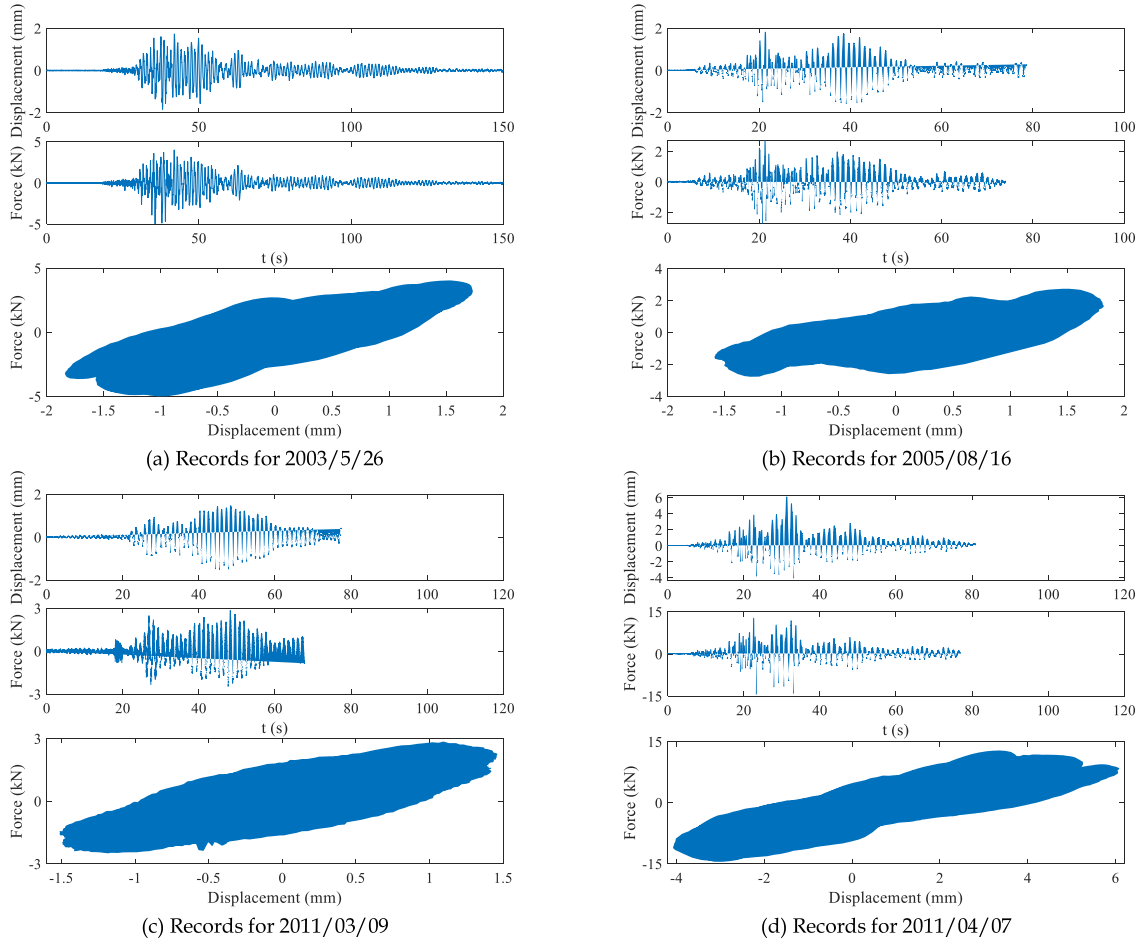


Fig. 6. Recorded data for damper force, displacement and hysteretic loop of novel oil dampers (Type II) in longitude direction.

dampers are illustrated in Fig.8.

The specifications about diameter and length of the orifices for 1st floor (Type I) and 3rd to 8th floor (Type II) are also shown in Fig.8. The stroke limits denote the extent of displacement that the pistons are able to move in horizontal direction, that is, 16 mm for 1st floor oil dampers (Type I) and 8 mm for 3rd to 8th floor oil dampers (Type II). Besides, in order to avoid the collision between the pistons and abutment which may happen under strong earthquake in extreme case, an extra cushion distance is preserved (8 mm for oil dampers of Type I and 5 mm for dampers of Type II). As can be observed from construction of oil damper in Fig.8, there are gaps between the cylinder and pistons which packed with viscoelastic polymer to allow for easy production. At the same time, the viscoelastic polymer constitutes soft rings serving to seal pressurized liquid, what's more, provides viscoelastic resisting force when the dynamic shear deformation enforces on sealing rings. Another main component of resistance force of the oil dampers is from inner pressure differential of liquid when oil flows through the narrow orifice.

Mathematical or physical models which can represent accurately the hysteretic behavior of the novel nonlinear oil dampers are essential for damper design, implementation, evaluation as well as future response prediction of such devices. In general, a series of dashpots and springs are most often utilized to express the mechanical characteristics of viscous damper devices, i.e., a Maxwell model. Since oil damper devices are implemented through braces or wall in most cases, thus, Maxwell model can represent both the stiffness



Fig. 7. Intact novel oil damper brace.

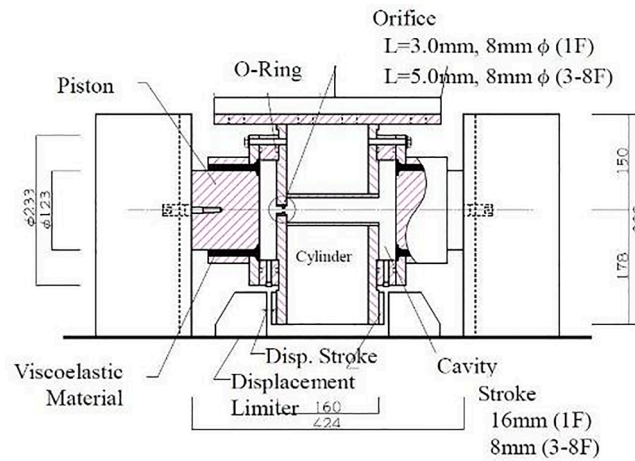


Fig. 8. Dimension of the novel oil damper.

provide by incorporated damper braces and the viscous dashpots.

The mathematical model for traditional oil damper brace has been considered as a linear viscous dashpot, therefore, the hysteretic behavior of traditional oil damper brace can be represented by a Maxwell model with a spring connected in series with a dashpot [2,10,25,27,29,30]. Nevertheless, the novel oil damper also produces viscoelastic resisting force by shear motion of sealing rings except the resisting force from inner pressure differential of fluid when oil flows through orifice. Therefore, analytical model for the novel oil damper brace incorporating the bracing frame is complicated and nonlinear. At the same time, the mathematical model for the novel oil damper brace is crucial to be incorporated into structural computational models, and for successful application in design practice, as well as for model updating and prediction using vibration data in structural health monitoring.

Studies have been done to investigate the dynamic behaviors of the novel oil dampers experimentally in small-scale implementations [28,31], which explicitly focus on the implementation of the novel oil dampers to mitigate seismic vibration of structures. In light of experimental observations, inner pressure differential when oil flows through orifice generates strong resisting force mainly under excitations with high frequency and large amplitude, while the resistance produced by the viscoelastic sealing rings are mostly corresponding to that of low frequency and small amplitude. The classical Maxwell models are capable of representing the frequency dependence of the damping and stiffness coefficients observed in orifice viscous dampers, while Kelvin-Voigt model is usually used to represent dynamic behavior of solid viscoelastic material, in which a dashpot and a spring are in parallel. Thence, three most probable model classes are investigated to try to account for the extent of stiffening and frequency dependence of the novel oil dampers, that is, the classical Maxwell models, the Kelvin-Voigt model and a combination complex model, in which a Kelvin solid is in parallel with a Maxwell fluid. Table 2. illustrates the simplified mechanical models and dynamic equilibrium equations of the three candidate model classes for the novel oil dampers.

3.2. Bayesian model selection methodology

3.2.1. Bayesian model selection

Bayesian model selection is employed to pick a most probable model which captures the main dynamic characteristics of the new type oil dampers and can also be used for predicting future response as well as reliability. Suppose recorded data for the new type oil dampers is as $\mathcal{D} \ominus = \{F_d, x_d\}$ which includes the measured damper force as output F_d and possibly the corresponding excitation displacement as input x_d . Take an assumption that a set of candidate model classes $\mathcal{M} = \cup \mathcal{M}_i$ ($i = 1, 2, 3, \dots, n_m$) are proposed for the new type oil dampers, in which n_m denotes the number of the considered candidate model classes. Then the relative probability of each input/output model class \mathcal{M}_i in the candidate model set based on data set $\mathcal{D} \ominus = \{F_d, x_d\}$ can be expressed by Bayes' Theorem as follows:

$$p(\mathcal{M}_i | \mathcal{D}, \mathcal{M}) = \frac{p(\mathcal{D} | \mathcal{M}_i) p(\mathcal{M}_i | \mathcal{M})}{p(\mathcal{D} | \mathcal{M})} \tag{3}$$

where $p(\mathcal{M}_i | \mathcal{M})$ is the prior probability specified by \mathcal{M}_i , and is utilized to express the initial plausibility of each model among the candidate models set. Noteworthy that the prior probability $p(\mathcal{M}_i | \mathcal{M})$ equals to $1/n_m$ when the probability model of prior model classes is taken equally plausible a priori. Then $p(\mathcal{D} | \mathcal{M}) = \sum_{i=1}^{n_m} p(\mathcal{D} | \mathcal{M}_i) p(\mathcal{M}_i | \mathcal{M}) = \frac{1}{n_m} \sum_{i=1}^{n_m} p(\mathcal{D} | \mathcal{M}_i)$, substituting both $p(\mathcal{D} | \mathcal{M})$ and the prior probability $p(\mathcal{M}_i | \mathcal{M}) = 1/n_m$ into equations (3) yields:

$$p(\mathcal{M}_i | \mathcal{D}, \mathcal{M}) = \frac{p(\mathcal{D} | \mathcal{M}_i)}{\sum_{i=1}^{n_m} p(\mathcal{D} | \mathcal{M}_i)} \tag{4}$$


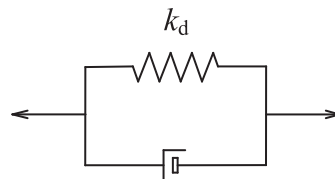
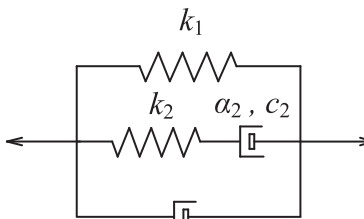
Therefore, the posterior probability $p(\mathcal{M}_i | \mathcal{D}, \mathcal{M})$ of each model class \mathcal{M}_i is directly determined by $p(\mathcal{D} | \mathcal{M}_i)$, where $p(\mathcal{D} | \mathcal{M}_i)$ is the normalizing constant, and is known as the evidence (or also referred to as marginal likelihood) for a model class \mathcal{M}_i given data set \mathcal{D} . Introducing the uncertain model parameters $\theta \in \mathbb{R}^{N_p}$, the evidence can then be given as follows:

$$p(\mathcal{D} | \mathcal{M}_i) = \int p(\mathcal{D} | \theta, \mathcal{M}_i) p(\theta | \mathcal{M}_i) d\theta \tag{5}$$

where $\theta \in \mathbb{R}^{N_p}$ is the uncertain parameter vector of each model in \mathcal{M}_i , N_p represents the dimension of the parameter vector. $p(\theta | \mathcal{M}_i)$ represents the prior probability of each model \mathcal{M}_i , which is chosen to quantify the initial probable of model class \mathcal{M}_i . $p(\mathcal{D} | \theta, \mathcal{M}_i)$ denotes the likelihood function which is defined as the probability function of obtaining data $\mathcal{D} \ominus = \{F_d, x_d\}$ given the probability density function $p(F_d | x_d, \theta, \mathcal{M}_i)$ with θ known.

3.2.1.1. Calculation of evidence for model classes. According to equation (4), the evidence $p(\mathcal{D} | \mathcal{M}_i)$ controls the corresponding posterior probability of model class \mathcal{M}_i , hence calculating the evidence for candidate model classes is crucial in model selection of the novel oil dampers. However, the calculation of the evidence in equation (5) through computing the multi-dimensional integral is nontrivial. For the cases that the proposed model class can be globally identified according to the available data $\mathcal{D} \ominus = \{F_d, x_d\}$, Laplace asymptotic approximation method is able to give an approximation for the evidence as follows [44,45]:

Table 2
Three candidate model classes for the novel oil dampers.

Maxwell model	Kelvin-Voigt model	Complex model
 <p style="text-align: center;">$k_d \quad \alpha_d, c_d$</p>	 <p style="text-align: center;">α_d, c_d</p>	 <p style="text-align: center;">α_1, c_1</p>
$\frac{\dot{F}_d(t)}{k_d} + \text{sign}(F_d(t)) \frac{F_d(t)}{c_d} ^{\alpha_d} = \dot{x}_d(t)$	$F_d(t) = k_d x_d(t) + \text{sign}(\dot{x}_d(t)) c_d \dot{x}_d(t) ^{\alpha_d}$	$\frac{\dot{F}_d(t) - k_1 \dot{x}_d(t) - \text{sign}(\dot{x}_d(t)) c_1 \alpha_1 \dot{x}_d(t) ^{\alpha_1 - 1}}{k_2} + \text{sign}(F_d(t) - k_1 x_d(t) - \text{sign}(\dot{x}_d(t)) c_1 \alpha_1 \dot{x}_d(t) ^{\alpha_1})^* \left \frac{F_d(t) - k_1 x_d(t) - \text{sign}(\dot{x}_d(t)) c_1 \alpha_1 \dot{x}_d(t) ^{\alpha_1}}{c_2} \right ^{1/\alpha_2} = \dot{x}_d(t)$

$$p(\mathcal{D}|\mathcal{M}_i) \approx p(\widehat{\boldsymbol{\theta}}|\mathcal{D}, \mathcal{M}_i)p(\widehat{\boldsymbol{\theta}}|\mathcal{M}_i)(2\pi)^{N_\theta/2}\det(H(\widehat{\boldsymbol{\theta}}))^{-1/2} \tag{6}$$

where N_θ denotes the dimension of model parameters $\boldsymbol{\theta}$ specified by the model class \mathcal{M}_i , $H(\boldsymbol{\theta})$ represents the Hessian matrix which equals to $-\ln[p(\mathcal{D}|\boldsymbol{\theta}, \mathcal{M}_i)p(\boldsymbol{\theta}|\mathcal{M}_i)]$ or $-\ln[p(\mathcal{D}|\boldsymbol{\theta}, \mathcal{M}_i)]$ for the maximum a posteriori (MAP) estimate or maximum likelihood estimate (MLE) of the model parameters $\boldsymbol{\theta}$, respectively.

For the cases that the proposed model class can't be globally identified on the basis of the available data $\mathcal{D} \ominus = \{\mathbf{F}_d, \mathbf{x}_d\}$, stochastic simulation methods, especially Markov Chain Monte Carlo algorithms, can be utilized to calculate the evidence of candidate model classes in practice. Following Bayes' Theorem, logarithmic form of the evidence in equation (5) can then be expressed as follows:

$$\begin{aligned} \ln[p(\mathcal{D}|\mathcal{M}_i)] &= \int \ln\left[\frac{p(\mathcal{D}|\boldsymbol{\theta}, \mathcal{M}_i)p(\boldsymbol{\theta}|\mathcal{M}_i)}{p(\boldsymbol{\theta}|\mathcal{D}, \mathcal{M}_i)}\right] p(\boldsymbol{\theta}|\mathcal{D}, \mathcal{M}_i) d\boldsymbol{\theta} \\ &= \int \ln[p(\mathcal{D}|\boldsymbol{\theta}, \mathcal{M}_i)] p(\boldsymbol{\theta}|\mathcal{D}, \mathcal{M}_i) d\boldsymbol{\theta} \\ &\quad - \int \ln\left[\frac{p(\boldsymbol{\theta}|\mathcal{D}, \mathcal{M}_i)}{p(\boldsymbol{\theta}|\mathcal{M}_i)}\right] p(\boldsymbol{\theta}|\mathcal{D}, \mathcal{M}_i) d\boldsymbol{\theta} \\ &= E[\ln(p(\mathcal{D}|\boldsymbol{\theta}, \mathcal{M}_i))] - E\left[\ln\left(\frac{p(\boldsymbol{\theta}|\mathcal{D}, \mathcal{M}_i)}{p(\boldsymbol{\theta}|\mathcal{M}_i)}\right)\right] \end{aligned} \tag{7}$$

where $E[\ln(p(\mathcal{D}|\boldsymbol{\theta}, \mathcal{M}_i))]$ is the expectation of the log likelihood function pertaining to the posterior $p(\boldsymbol{\theta}|\mathcal{D}, \mathcal{M}_i)$, which measures the average data-fit for the model class \mathcal{M}_i . $E\left[\ln\left(\frac{p(\boldsymbol{\theta}|\mathcal{D}, \mathcal{M}_i)}{p(\boldsymbol{\theta}|\mathcal{M}_i)}\right)\right]$ represents the Kullback–Leibler information, also called as relative entropy in information theory [46], which measures the information gain for the model class \mathcal{M}_i from the available data $\mathcal{D} \ominus = \{\mathbf{F}_d, \mathbf{x}_d\}$ and is always non-negative.

3.2.1.2. Choice of prior and Likelihood function. Before calculating the evidence and posterior probability of each model classes, prior probability model $p(\boldsymbol{\theta}|\mathcal{M}_i)$ is chosen as a Gaussian prior which generates the largest prior uncertainty for the model parameters $\boldsymbol{\theta}$ by Jaynes' Principle of Maximum (Information) Entropy [47]. The Gaussian prior can be expressed as follows:

$$p(\boldsymbol{\theta}|\mathcal{M}_i) = \mathcal{N}(0, \sigma_\theta^2 I) = \frac{1}{(2\pi\sigma_\theta^2)^{(N_\theta-1)/2}} \exp\left[-\frac{1}{2} \frac{\boldsymbol{\theta}^T \boldsymbol{\theta}}{\sigma_\theta^2}\right] \tag{8}$$

where σ_θ^2 is the specified upper bound of prior variance for each component of the parameters vector $\boldsymbol{\theta}$.

Furthermore, the likelihood function can be defined as function of the model prediction error $\varepsilon = F_d - \widehat{F}_d$ which measures the agreement between the measured and predicted response, once parameter vector $\boldsymbol{\theta}$ is available. Since Gaussian probability models can generate the most uncertainty (largest Shannon entropy) in the prediction-error time history stated by Jaynes' Principle of Maximum (Information) Entropy [47], thus, suppose that the prediction error ε is a discrete zero-mean Gaussian distribution, that is, $\varepsilon \sim N(0, \Sigma) = N(0, \sigma_j^2 I)$, in which Σ represents the covariance matrix, σ_j^2 denotes the j th variance of the prediction error, and I is an identity matrix. Finally, the likelihood function could be determined by the prediction error as follows:

$$p(\mathcal{D}|\boldsymbol{\theta}, \mathcal{M}_i) = p(\mathbf{F}_d|\mathbf{x}_d, \boldsymbol{\theta}, \mathcal{M}_i) = \prod_{j=1}^{N_m} \frac{1}{(\sqrt{2\pi\sigma_j^2})^N} \exp\left(-\sum_{j=1}^{N_m} \sum_{n=1}^N \frac{1}{2\sigma_j^2} (F_{d,j}(t_n) - \widehat{F}_{d,j}(t_n))^2\right) \tag{9}$$

where N_m represents the dimension of measurement vectors, N denotes the number of data in each measurement vector, $F_{d,j}(t_n)$ and $\widehat{F}_{d,j}(t_n)$ are the measured and corresponding estimated system output response for the j th measurement at t_n .

Table 3
Posterior probability of candidate model classes for the novel oil dampers.

Records	Direction	Damper type	Model class	Log evidence	Data-fit	Information gain	Posterior probability
2003/5/26	EW	Damper I	\mathcal{M}_1	-40.5	-30.5	10.1	0.0
			\mathcal{M}_2	1064.9	1086.6	21.6	1.0
			\mathcal{M}_3	249.7	284.5	34.7	0.0
		Damper II	\mathcal{M}_1	103.6	114.1	10.5	0.0
			\mathcal{M}_2	8.9	17.7	8.9	0.0
			\mathcal{M}_3	4433.6	4481.3	47.7	1.0
	NS	Damper I	\mathcal{M}_1	-74.4	-64.7	9.6	4.2e-270
			\mathcal{M}_2	546.0	564.8	18.9	1.0
			\mathcal{M}_3	412.0	441.5	29.5	6.7e-59
		Damper II	\mathcal{M}_1	-335.7	-326.6	9.1	0.0
			\mathcal{M}_2	105.4	122.1	16.7	0.0
			\mathcal{M}_3	5328.3	5379.0	50.8	1.0

3.3. Determining model of the novel oil dampers

Implementing above Bayesian model selection approaches to actual recorded data of the novel oil dampers obtained from the vibration monitoring system on dampers described in the previous sections, three most probable model classes are investigated, that is, the classical Maxwell models, the Kelvin-Voigt model and a combination complex model, in which a Kelvin solid is in parallel with a Maxwell fluid. The three model classes for the novel oil dampers are referred to as $\mathcal{M}_1, \mathcal{M}_2$ and \mathcal{M}_3 , respectively. Finally, the posterior probability of each candidate model class of the novel oil dampers is obtained. Take the recorded data on 26th May 2003 as an example of analysis, Table 3 lists the log evidence, date-fit, information gain, as well as the posterior probability of candidate model classes for the novel oil dampers (Type II and Type I) in both longitude (EW) and transverse (NS) direction.

From the results of Bayesian model selection in Table 3, the model class \mathcal{M}_3 shows the best date-fit, largest information gain and log evidence, which obvious precedes the other model classes for the novel oil dampers Type II. In addition, the posterior probability of the model class \mathcal{M}_3 is one hundred percentage, indicating itself the dominated model class among these candidate model classes. While the model class \mathcal{M}_2 displays the best date-fit for the novel oil dampers Type I, nevertheless, selecting a model class merely according to the data-fit term in equation (7) may bring about over-fitting problem of the data which may result in poor subsequent response predictions or even be unreliable by the selected model class due to taking too much detail information from the specific data. Besides, more complex models prefer over simpler models based on the data-fit term.

On the contrary, Ockham’s razor states that simpler models prefer over more complex models, if the simpler models produce reasonably consistency with the data, and just slightly worse than the complex models. The log evidence for \mathcal{M}_i in equation (7) explicitly establish such a trade-off between the information-theoretic complexity and data-fit of the model class, and builds in a penalty against complex models in this sense. Therefore, the best model class for nonlinear oil dampers Type I is determined through competing the posterior probability of each model class as shown in Table 3. Moreover, the determined best model classes for different seismic records are listed in Table 4.

4. Identification of nonlinear oil dampers by PF-MCMC

4.1. PF-MCMC Bayesian identification methodology

4.1.1. Particle filtering algorithm

In this section, a general overview of the particle filtering methodology will be described. For more detailed theoretical derivation, the reader is referred to [48,49]. Particle filtering (PF) belongs to a kind of sequential Monte Carlo method, whose main idea lies in using a set of random samples and associated weights to express the required posterior probability density function. With the increase of the number of samples, the set of random samples approximate sequentially to actual probability density function of the target distribution.

For the sake of generality, consider the generalized dynamical system which can be expressed in discrete state space form as follows:

$$x_k = f(x_{k-1}) + w_k \tag{10}$$

$$y_k = h(x_k) + v_k \tag{11}$$

where equation (10) is the discrete state space equation, which is also referred to as process equation, while equation (11) is the observation equation, which is also referred to as measurement equation. x_k represents the state variable vector at $t = k\Delta t$, Δt is the sampling time, k denotes time step. w_k is the process noise vector following the Gaussian distribution with covariance matrix Q_k , i.e. $w_k \sim N(0, Q_k)$, and is utilized to model noise in measured inputs, non-parametric model errors and/or unmeasured inputs. y_k represents the observation vector at time step k . v_k is the observation noise vector following the Gaussian distribution with corresponding covariance matrix R_k , i.e. $v_k \sim N(0, R_k)$, and is utilized to model noise in the measurement.

In practice, the general problem encountered for nonlinear dynamical system is to estimate the latent state vector x_k given the measurements $y_{1:k}$, that is, the posterior probability density $p(x_k|y_{1:k})$ is desired, and can be expressed by Bayes’ theorem as follows:

$$p(x_k|y_{1:k}) = \frac{p(y_k|x_k)p(x_k|y_{1:k-1})}{p(y_k|y_{1:k-1})} \tag{12}$$

Employing the Chapman–Kolmogorov theorem, above equation (12) can be rewritten as follows:

Table 4
Determined best model classes under different seismic records.

Damper type	Direction	2003/5/26	2005/8/16	2011/3/9	2011/4/7
Damper I	EW	\mathcal{M}_2	\mathcal{M}_3	\mathcal{M}_2	\mathcal{M}_2
	NS	\mathcal{M}_2	\mathcal{M}_3	\mathcal{M}_2	\mathcal{M}_2
Damper II	EW	\mathcal{M}_3	\mathcal{M}_3	\mathcal{M}_3	\mathcal{M}_3
	NS	\mathcal{M}_3	\mathcal{M}_3	\mathcal{M}_3	\mathcal{M}_3

$$p(x_k|y_{1:k}) = \frac{p(y_k|x_k) \int p(x_k|x_{k-1}, y_{1:k-1})p(x_{k-1}|y_{1:k-1})dx_{k-1}}{p(y_k|y_{1:k-1})} = \frac{p(y_k|x_k) \int p(x_k|x_{k-1})p(x_{k-1}|y_{1:k-1})dx_{k-1}}{p(y_k|y_{1:k-1})} \tag{13}$$

where $p(x_k|x_{k-1})$ represents Markovian transitional probability density, also referred to as state evolution of the system, and $p(y_k|x_k)$ denotes its emission probability density. $y_{1:k}$ is the whole set of observations (y_1, y_2, \dots, y_k) . In addition, take an assumption that the process equation is a first-order Markov process, and is independent of the observations, i.e., $p(x_k|x_{k-1}, y_{1:k-1}) = p(x_k|x_{k-1})$.

Then, the recursive estimation of posterior distribution density can be obtained through introducing the normalized weights as follows:

$$\hat{p}(x_k|y_{1:k}) = \sum_{i=1}^{N_s} W_k^{(i)} \delta(x_k - x_k^{(i)}) \tag{14}$$

Furthermore, the marginal likelihood $p(y_{1:k})$ can also be estimated through above particle filtering algorithm by

$$\hat{p}(y_{1:k}) \triangleq \hat{p}(y_1) \prod_{n=2}^k \hat{p}(y_n|y_{1:n-1}) \tag{15}$$

In which

$$\hat{p}(y_k|y_{k-1}) = \frac{1}{N_s} \sum_{i=1}^{N_s} W_k(x_k^{(i)}) \tag{16}$$

4.1.1.1. Resampling and sample impoverishment. In general, with the increase of the number of particles, the estimated $p(x_k|y_{1:k})$ by equation (14) approximates the true posterior density. Nevertheless, a common problem encountered is particles degeneracy in the process of particle filtering implementation. Particles degeneracy denotes the phenomenon of obviously uneven distributed particles which only a few particles possess significant weights after some iterative steps, which consumes considerable computational effort to update the particles of ‘trivial’ contribution to the estimated $p(x_k|y_{1:k})$. The effective samples size is then introduced to measure the degeneracy, and can be estimated by the particle weights variance as follows [50]:

$$N_{eff} = \frac{1}{\sum_{i=1}^{N_s} (W_k^{(i)})^2} \tag{17}$$

The sample degeneracy problem can be alleviated by resampling. The resampling procedure replaces the particles of negligible weights with duplicated particles of larger weights. Whenever N_{eff} drops below pre-defined threshold value, implement the resampling procedure. Thus, a new set of samples $\{x_k^{i,*}, i = 1, \dots, N_s\}$ is generated with $Pr(x_k^{i,*} = x_k^j) = W_k^j$, where x_k^j is the particle of the largest weights.

However, new issue occurs to the particles due to a loss of diversity, as the set of resultant samples involves a lot of duplicated particles for certain given weights, which is referred to as sample impoverishment (also called particle depletion). The sample impoverishment becomes especially notable for small process noise cases [51,52]. Besides, no particles in the vicinity of the true state may happen as the particles propagate iteratively, even for a large number of particles. Several existing techniques have been exploited to tackle or diminish the sample impoverishment problem, e.g. regularization, the resample-move algorithm [53-57]. Among them, Markov Chain Monte Carlo (MCMC) algorithm is capable of handling complicated probability density functions (PDFs), for example, large tail probabilities, peaked PDFs and multimodal PDFs.

4.2. PF-MCMC approach

To cope with the particle degeneracy, resampling scheme is adopted to substitute the particles of low weights with replicated particles of high weight, then, the resampled particles are reset to focus on high likelihood regions at each iterative step. Though avoiding the degeneracy issue in this way, bringing about another problem of particle depletion. In this section, MCMC steps are exploited in particle filters to form a PF-MCMC approach, which not only circumvents the problem of particle depletion, but also constructs an efficient proposal distribution even for high dimension.

Nonetheless, the coalescence of particle filter and MCMC algorithm is non-trivial. What’s more, both the parameters and states are needed to be estimated given the observations in practice for most cases. A common way is to joint estimate the parameters and states by augmenting the parameters into state vector. Particle filtering method is then implemented over the augmented space, which aggravates the sample impoverishment problem. The prerequisite assumption for the PF to be stable is that the system is fast mixing, which indicates the state x_k is roughly independent of one step previous state x_{k-1} for a relatively small lag. While the prerequisite is no longer hold any more, since the parameters are constant in the augmented state without variation in time. One possible way to mitigate this issue is to put in a random-walk noise on each parameter. Nevertheless, this can lead to issues of convergence and accuracy if the noise level is not appropriately calibrated.

In this section, an approach to decouple the augmented state and parameter joint estimation problem is proposed and implemented in two sequential phases for one iterative step as follows: a Bayesian parameter identification phase in which only the model pa-

rameters are estimated through MCMC algorithm, and a state estimation phase where particle filter is utilized to estimate the model state. To successfully realize above proposed approach, re-parameterizing the parameters posterior PDF is necessary to incorporate the state predictive distribution. Consider the generalized dynamical system described by equations (10)- (11) in previous section with parameters unknown, which can be rewritten as below equations (18)- (19), moreover, the posterior PDF of parameters vector θ which parameterizes the dynamic model can be inferred from the noise contaminated measurements by Bayes' theorem as follows:

$$x_k = f(x_{k-1}, \theta) + w_k \tag{18}$$

$$y_k = h(x_k, \theta) + v_k \tag{19}$$

$$p(\theta|y_{1:k}) = \frac{p(y_{1:k}|\theta)p(\theta)}{p(y_{1:k})} \tag{20}$$

where $p(\theta)$ denotes the prior distribution of parameters vector θ , which represents the prior knowledge about the parameters given the information available before the data collection, $p(y_{1:k}|\theta)$ is the likelihood function, and $p(y_{1:k})$ is a normalizing constant.

In Bayesian inference, the posterior PDF of parameters vector θ is the desired target, where the parameters vector θ completely or partially defines the system model. To calculate the parameters posterior $p(\theta|y_{1:k})$ recursively, the likelihood function $p(y_{1:k}|\theta)$ can be rewritten as follows [58,59]:

$$\begin{aligned} p(y_{1:k}|\theta) &= p(y_{1:k-1}, y_k|\theta) = p(y_k|y_{1:k-1}, \theta)p(y_{1:k-1}|\theta) \\ &= p(y_{1:k-1}|\theta) \int p(x_k, y_k|y_{1:k-1}, \theta)dx_k \\ &= p(y_{1:k-1}|\theta) \int p(y_k|x_k, \theta)p(x_k|y_{1:k-1}, \theta)dx_k \end{aligned} \tag{21}$$

where $p(y_k|x_k, \theta)$ is defined by the measurement equation (24), while $p(x_k|y_{1:k-1}, \theta)$ is defined by the state evolution equation (23) of the dynamic system, also referred to as the state predictive probability distribution. Implementing the recursive expansion of $p(y_{1:k-1}|\theta)$ in turn, the likelihood function can then be expressed by

$$p(y_{1:k}|\theta) = \prod_{i=1}^N \int p(y_i|x_i, \theta)p(x_i|y_{1:i-1}, \theta)dx_i \tag{22}$$

where N represents the number of recorded data in measurement vector y , in addition, above equation (22) alludes the fact that the current measurement given the state doesn't depend on the past measurements.

Take the initial condition $p(x_1|y_0, \theta) = p(x_1|\theta)$, substituting the likelihood function expressed by equation (22) into equation (20) yields:

$$p(\theta|y_{1:k}) \propto p(\theta) \prod_{i=1}^N \int p(y_i|x_i, \theta)p(x_i|y_{1:i-1}, \theta)dx_i \tag{23}$$

To calculate the state predictive distribution $p(x_i|y_{1:i-1}, \theta)$, state estimation methods are employed. In Bayesian inference, the state estimation methods are generally aiming to recursively estimate the state posterior $p(x_i|y_{1:i}, \theta)$, when uncertain parameters vector is fixed at the time being. Following the Bayes' theorem, the state posterior $p(x_i|y_{1:i}, \theta)$ can then be expressed as follows:

$$p(x_i|y_{1:i}, \theta) = \frac{p(y_i|x_i, \theta)p(x_i|y_{1:i-1}, \theta)}{p(y_i|y_{1:i-1}, \theta)} \tag{24}$$

Here, given that uncertain parameters vector is fixed, above equation (29) is actually equivalent to equation (12). While the state predictive distribution $p(x_i|y_{1:i-1}, \theta)$ can be acquired through the projection of the posterior $p(x_{i-1}|y_{1:i-1}, \theta)$ at the previous time step as follows:

$$p(x_i|y_{1:i-1}, \theta) = \int p(x_i|x_{i-1}, \theta)p(x_{i-1}|y_{1:i-1}, \theta)dx_{i-1} \tag{25}$$

In general, above integral in equation (25) is intractable in addition to some special cases with linear Gaussian assumption. Besides, there are no closed form solutions about the state posterior $p(x_{i-1}|y_{1:i-1}, \theta)$ for dynamic system of non-linear non-Gaussian models. Therefore, there is no analytical expression for the state predictive distribution $p(x_i|y_{1:i-1}, \theta)$ for non-linear non-Gaussian models. Approximations methods are adopted to tackle this difficulty. Sequential Monte Carlo (SMC) methods have been proven to be capable of providing approximations to the state posterior $p(x_{i-1}|y_{1:i-1}, \theta)$, e.g. sequential important resampling particle filter algorithm. Take an assumption that sampling from the state probability density conditional on previous measurements, $p(x_i|y_{1:i}, \theta)$, is feasible for any $\theta \in \mathbb{R}^{Np}$, and joint the parameters and states probability density conditional on the measurements, $p(\theta, x_i|y_{1:i})$ is then decomposed as $p(\theta, x_i|y_{1:i}) = p(x_i|y_{1:i}, \theta)p(\theta|y_{1:i}) = p(\theta|y_{1:i})p_\theta(x_i|y_{1:i})$. Hence, the following density distribution can be used as a proposal of Metropolis-Hastings sampler for particles update. The proposal density can be expressed as follows [60]:

$$q\{(\theta^*, x_i^*) | (\theta, x_i)\} = q(\theta^* | \theta) p_{\theta^*}(x_i^* | y_{1:i}) \tag{26}$$

where θ^* and x_i^* are the proposed samples for parameters vector θ and states x_i , while the dimension of the algorithm is determined by $q(\theta^* | \theta)$, which will significantly affect the algorithm’s performance. The acceptance ratio is then calculated as follows:

$$\text{Acceptance ratio} = \frac{p(\theta^*, x_i^* | y_{1:i})}{p(\theta, x_i | y_{1:i})} \frac{q\{(\theta, x_i) | (\theta^*, x_i^*)\}}{q\{(\theta^*, x_i^*) | (\theta, x_i)\}} = \frac{p_{\theta^*}(y_{1:i}) p(\theta^*) q(\theta | \theta^*)}{p_{\theta}(y_{1:i}) p(\theta) q(\theta^* | \theta)} \tag{27}$$

where the marginal density $p(\theta | y_{1:i})$ is proportional to density $p_{\theta}(y_{1:i}) p(\theta)$, which is the effectively targets of the algorithm implied in above acceptance ratio expression equation (27), as the proposal density transfers taking samples from the joint density $p(\theta, x_i | y_{1:i})$ into sampling from marginal density $p(\theta | y_{1:i})$, from which it is much easier to draw samples. Particle filter approximation is exploited in the Metropolis–Hastings update, where the output particles of the particle filter algorithm aiming at $p_{\theta}(x_i | y_{1:i})$ is exploited as a proposal. Furthermore, the estimated marginal density $\hat{p}(y_{1:i})$ by equation (15) is used instead for the calculation of the acceptance ratio in equation (27).

Thus, the parameters posterior density $p(\theta | y_{1:k})$ and the state posterior density $p(x_i | y_{1:i}, \theta)$ are computed, and the resulted posterior estimates can be expressed as $\hat{\theta}(y_{1:k})$ and $\hat{x}_i(y_{1:i}, \theta)$, respectively. Finally, following the Theorem of Total Probability, the state prediction can be achieved and written as follows:

$$p(x_i | y_{1:i}) = \int p(x_i | y_{1:i}, \theta) p(\theta | y_{1:k}) d\theta \approx \int p(\hat{x}_i | y_{1:i}, \theta) p(\hat{\theta} | y_{1:k}) d\theta \tag{28}$$

After all, the proposed PF-MCMC approach circumvents the problem of state augmentation, and reduces the numerical instability and ill-posedness of the algorithm incurred by complex topology of the augmenting state and highly nonlinearity. Besides, the decoupling of state augmentation may enhance conditions of identifiability allowing for high dimensional parameters to be estimated. In the process of PF-MCMC, particle filtering methods are targeting only states density $p_{\theta}(x_i | y_{1:i})$, which is less likely to suffer from the particle depletion. Moreover, the combination of an MCMC algorithm with particle filters proposes new samples enriching the diversity of particles, and is capable of efficiently draw samples from general difficulty probability density functions (PDFs), e.g. multi-modal PDFs, non-linear non-Gaussian PDFs, large tail PDFs, and peaked PDFs when the number of data is adequately large. In summary, a generic PF-MCMC algorithm is then illustrated as follows:

PF-MCMC algorithm

Select the number of iterations N_{mcmc} for MCMC samplers

Initialization: $j = 1$

Select the prior distribution of parameters, $p(\theta)$, and set $\theta(j = 1)$ arbitrarily

Set the number of samples N_s and run a particle filtering algorithm targeting $p_{\theta(j=1)}(x_i | y_{1:i})$ for all $i = 1 : T$ using equations. (14) - (15), take particles $X_{1:T}(j = 1) \sim \hat{p}_{\theta(j=1)}(\cdot | y_{1:T})$, and take $\hat{p}_{\theta(j=1)}(y_{1:T})$ as the estimates of the marginal likelihood.

Calculate $p(\theta(j = 1) | y_{1:T})$ and $p_{(j=1)}(\hat{x}_{1:T} | y_{1:T})$ by equation (23) and (27), respectively.

Iteration: while $j = 2 : N_{mcmc}$

Propose a move to $\theta(j)$ from proposal distribution $q\{\cdot | \theta(j - 1)\}$, i.e. sample $\theta^* \sim q\{\cdot | \theta(j - 1)\}$,

run a particle filtering algorithm targeting $p_{\theta^*}(x_i | y_{1:i})$ for all $i = 1 : T$ using equations. (14) - (15), take particles $X_{1:T}^* \sim \hat{p}_{\theta^*}(\cdot | y_{1:T})$, and take $\hat{p}_{\theta^*}(y_{1:T})$ as the estimates of the marginal likelihood.

Compute logarithm of the acceptance ratio as follows:

$$\log(\alpha^j) = \min\left\{ \log(1), \log\left(\frac{\hat{p}_{\theta^*}(y_{1:T}) p(\theta^*) q\{\theta(j - 1) | \theta^*\}}{\hat{p}_{\theta(j-1)}(y_{1:T}) p\{\theta(j - 1) | \theta^*\} q\{\theta^* | \theta(j - 1)\}}\right) \right\}$$

Generate a variate $u \sim \text{uniform}[0, 1]$

If $\log(u) < \log(\alpha^j)$,

Accept the proposed move and take $\theta(j) = \theta^*$, $X_{1:T}^{(j)} = X_{1:T}^*$, and $\hat{p}_{\theta(j)}(y_{1:T}) = \hat{p}_{\theta^*}(y_{1:T})$;

otherwise

Let $\theta(j) = \theta(j - 1)$, $X_{1:T}^{(j)} = X_{1:T}^{(j-1)}$, and $\hat{p}_{\theta(j)}(y_{1:T}) = \hat{p}_{\theta(j-1)}(y_{1:T})$

Calculate $p(\hat{\theta}(j) | y_{1:T})$ and $p_{(j)}(\hat{x}_{1:T} | y_{1:T})$ by equation (23) and (28), respectively.

End

In above process, the proposed PF-MCMC algorithm is iterated recursively until j reaches the pre-set number of iterations, N_{mcmc} . T represents the length of measurement y . In general, it takes some times before Markov Chain converge to true target posterior probability density, which has been referred to as “burn-in” period. Thus, it’s practical to monitor the acceptance ratio so as to make sure the convergence of Markov Chain, and the acceptance ratio works well within [0.15 0.4] for practical application.

4.3. Implementation of identifying nonlinear oil dampers

In this section, the proposed PF-MCMC approach is exploited to identify the nonlinear oil dampers based on the model class selected in section 3. The nonlinear oil dampers compose of a cylinder and a pair of pistons, and there is a gap between cylinder and piston, packing with viscoelastic polymer, which make soft rings to allow relative motion between the pistons and cylinder, and to serve to seal

pressurized fluid. The nonlinear oil dampers are connected through the V-type steel braces between the adjacent floors. The pair of pistons are installed in the U-type abutment which is fixed on the floor, while the central cylinder is mounted onto the V-type brace, as shown in as in Fig.7. Thus, the central cylinder moves relative to the pistons back and forth in horizontal direction. Two types of nonlinear oil dampers with different orifice specifications and stroke limits of relief mechanism are utilized for 1st floor (Type I) and 3rd to 8th floor (Type II), respectively.

Analytical models which can represent accurately the hysteretic behavior of the novel nonlinear oil dampers are essential for damper design, implementation, evaluation as well as future response prediction of such devices. From the result of Bayesian model selection, a combination complex model has been proven to be capable of better describing the dynamic behavior of the nonlinear oil dampers, in which a Kelvin solid is in parallel with a Maxwell fluid. Schematic diagram of the complex model is then illustrated in Fig. 9. The dynamic equilibrium equation of the nonlinear oil damper brace for the complex model can be expressed as follows:

$$\frac{\dot{F}_d(t) - k_1 \dot{x}_d(t) - \text{sign}(\dot{x}_d(t)) c_{d1} \alpha_{d1} \left| \dot{x}_d(t) \right|^{\alpha_{d1}-1}}{k_2} + \text{sign}(F_d(t) - k_{d1} x_d(t)) - \text{sign}(\dot{x}_d(t)) c_{d1} \left| \dot{x}_d(t) \right|^{\alpha_{d1}} \left| \frac{F_d(t) - k_{d1} x_d(t) - \text{sign}(\dot{x}_d(t)) c_{d1} \left| \dot{x}_d(t) \right|^{\alpha_{d1}}}{c_{d2}} \right|^{1/\alpha_{d2}} = \dot{x}_d(t) \tag{29}$$

where $F_d(t)$ denotes the axial force of the oil damper brace, and $x_d(t)$ is the displacement of the oil damper brace. k_{d1} and k_{d2} are the stiffness coefficient, c_{d1} and c_{d2} are the viscous damping coefficient, α_{d1} and α_{d2} are the corresponding velocity exponent, which is dictated by the property of the viscous liquid and designed dimension of the orifice. The sign (\cdot) denotes the signum function. Since the complex model is actual a combination of a Kelvin solid in parallel with a Maxwell fluid, the set of coefficient, k_{d1}, c_{d1} and α_{d1} , can be considered as the parameters of Kelvin-Voigt model, meanwhile, k_{d2}, c_{d2} and α_{d2} can be considered as the parameters of Maxwell model.

The proposed PF-MCMC algorithm is implemented to identify the model of the nonlinear oil damper, which re-parameterizes the joint posterior parameters and states distribution to decouple the parameters and states estimation. A main feature of the PF-MCMC algorithm is that it can be applicable to non-Gaussian distributions, which limits the application of Kalman filtering series methods. Prior information about the parameters and states of the nonlinear oil damper is general available before data collection. Then, the prior distributions of parameters are selected based on the knowledge of structural drawings, design specifications, in-site construction, as well as information available in common engineering practice. Thus, the parameters prior distributions are chosen as uniform distributions and independent with each other. To make sure that the parameter space is explored evenly for each parameter, all parameters are leveraged to similar orders of magnitude. Detailed settings of the prior parameters are as follows: $k_{dn}/1000 \sim U(0.01, 10)$, $c_{dn}/100 \sim U(0.01, 10)$, $\alpha_{dn} \sim U(0.5, 1.5)$, where $n = 1, 2$, U represents uniform distribution.

In this case, the state vector of the nonlinear oil damper can be established and expressed as follows:

$$X = [x, \dot{x}]^T = [x_1, x_2]^T \tag{30}$$

Based on equations (23) and (34), the discrete state transition equation can then be expressed as follows:

$$f(x_k, \ddot{x}_{floor}) = x_{k-1} + \int_{(k-1)\Delta t}^{k\Delta t} f(x_{k-1}, \ddot{x}_{floor}) + w_k \tag{31}$$

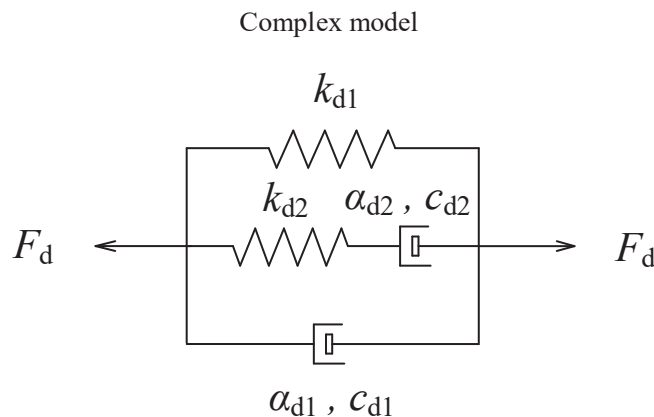


Fig. 9. Schematic diagram of complex model.

where

$$f \begin{pmatrix} x_{k-1}, \ddot{x}_{floor} \end{pmatrix} = \begin{bmatrix} \dot{x}_1 \\ \dot{x}_2 \end{bmatrix} = \begin{bmatrix} x_2 \\ \left(\frac{\left(\dot{F}_d(t) - k_{d1}x_2 - k_{d2} \left(x_2 - \text{sign}(F_d(t) - k_{d1}x_1 - \text{sign}(x_2)c_{d1}|x_2|^{\alpha_{d1}}) \left| \frac{F_d(t) - k_{d1}x_1 - \text{sign}(x_2)c_{d1}|x_2|^{\alpha_{d1}}}{c_{d2}} \right|^{1/\alpha_{d2}} \right) \right)}{\text{sign}(x_2)c_{d1}\alpha_{d1}} \right)^{\frac{1}{\alpha_{d1}-1}} \end{bmatrix} \quad (32)$$

In a similar way, the discrete observation equation can then be defined as follows:

$$h \begin{pmatrix} x_k, \ddot{x}_{floor} \end{pmatrix} = \begin{bmatrix} x_1 \\ \left(\frac{\left(\dot{F}_d(t) - k_{d1}x_2 - k_{d2} \left(x_2 - \text{sign}(F_d(t) - k_{d1}x_1 - \text{sign}(x_2)c_{d1}|x_2|^{\alpha_{d1}}) \left| \frac{F_d(t) - k_{d1}x_1 - \text{sign}(x_2)c_{d1}|x_2|^{\alpha_{d1}}}{c_{d2}} \right|^{1/\alpha_{d2}} \right) \right)}{\text{sign}(x_2)c_{d1}\alpha_{d1}} \right)^{\frac{1}{\alpha_{d1}-1}} \end{bmatrix} + v_k \quad (33)$$

In which the simultaneous observation vectors are the absolute acceleration $\ddot{x} + \ddot{x}_{floor}$ and relative displacement x of the nonlinear oil dampers. The relative displacement x is recorded by the LVDT as shown in Fig. 5. The floor accelerations, \ddot{x}_{floor} , are also measured by the accelerometers installed on floors from the structural health monitoring system of the building.

Take an assumption that all states and observations are independent with each other, hence, the corresponding process noise covariance matrices (Q) is a 2×2 diagonal matrix, in which only diagonal elements q_{11} and q_{22} are non-zero. Similarly, the measurement noise covariance matrix (R) is a 2×2 diagonal matrix, in which only diagonal elements r_{11} and r_{22} are non-zero. Besides, assume that the corresponding measurement noise covariance r_{11}, r_{22} and process noise covariance q_{11}, q_{22} are inverse gamma distribution. The model error equals to the difference between the measured damper force and damper force produced by the selected model for the nonlinear oil damper. Gaussian likelihood function is then adopted to describe the distribution of model error. The Gaussian likelihood function can hence then be defined as follows:

$$p(F_d(t)|x_d(t)) = \frac{1}{\sqrt{2\pi R^2}} \exp \left[-\frac{(F_d(t) - \bar{F}_d(t))^2}{2R} \right] \quad (34)$$

where $F_d(t)$ is the measured observation vector and $\bar{F}_d(t)$ represents the corresponding predicted damper force vector based on available prior information.

4.4. Parameter analysis and identification results

In this section, the dynamic characteristics for the nonlinear oil dampers are about to be evaluated using the identification results by the proposed PF-MCMC algorithm. In order to investigate actual performance and dynamic characteristics of the new type of oil dampers, both the structural health monitoring system of the building and vibration monitoring system for the nonlinear oil damper were instrumented, respectively. As shown in Fig. 8, one end of displacement-meter was mounted on the oil damper, while the other end was placed on the floor, thus, the relative axial displacement of the oil damper brace was obtained following the track direction. Strain gauges were also deployed to measure axial forces of the oil damper braces. The distribution of load cell gauge and displacement transducers on the oil damper is depicted as in Fig.5. Besides, the vibration monitoring system has been instrumented on the dampers since 2003, and the vibration monitoring system has accumulated large amount of valuable date. Among them, the recorded earthquakes with magnitude greater than 7 were employed to train and predict the model response of the nonlinear oil damper braces. Table 1 lists the detail specifications of these selected earthquake records.

Furthermore, the recordings on May 26th 2003 were utilized to estimate the model parameters and train a generic model for the nonlinear oil dampers, which captures the main characteristics and is capable of successfully simulating the dynamic behavior of the nonlinear oil dampers. Then, data records for 2005/08/16, 2011/03/09 and 2011/04/07 are employed to validate and evaluate the identified model. There are two kinds of nonlinear oil dampers with different orifice specifications and stroke limits of relief mechanism, which are utilized for 1st floor (Type I) and 3rd to 8th floor (Type II), respectively. As the identification and evaluation procedure are similar for oil dampers of Type I and II, herein, take a detailed analysis of oil damper Type II as an example. The recorded data about damper force, displacement and hysteretic behavior for oil dampers (Type II) in longitude direction are also displayed in Fig.6, which will be used for further analysis.

The main response of the nonlinear oil damper happens during a segment period from 15 s to 60 s, which includes the maximum response. Hence, the segment period from 15 s to 60 s is utilized to estimate the model of the nonlinear oil damper for both longitudinal and transverse directions of the building (corresponding to east–west (EW) and north–south (NS) directions). The sampling interval of

the recorded signals is 0.005 s. Recall that the input vector is the relative displacement x , and the output vector is the damper force for the complex model of the nonlinear oil dampers, $k_{d1}, k_{d2}, c_{d1}, c_{d2}, \alpha_{d1}, \alpha_{d2}$ are uncertain parameters, whose prior distributions are chosen as follows: $k_{dn}/1000 \sim U(0.01, 10)$, $c_{dn}/100 \sim U(0.01, 10)$, and $\alpha_{dn} \sim U(0.5, 1.5)$, where $n = 1, 2$. To reduce the effect of parameter initial value, 1000 sets of initial parameter samples are generated randomly. The initial values for the dynamic states of the nonlinear oil damper are assumed to be 0. Then, the proposed PF-MCMC algorithm is conducted to the nonlinear oil dampers starting from the 1000 sets of initial parameter samples.

The posterior parameter distribution of identified complex model are illustrated in Fig. 10 and Fig. 11 for the longitudinal and transverse directions, respectively. As can be observed from the identification results of posterior parameter probability distribution, the posterior distributions for each uncertain parameter, $k_{d1}, k_{d2}, c_{d1}, c_{d2}, \alpha_{d1}, \alpha_{d2}$, are generally tight within a narrow band, and the variance for each uncertain parameter is also relatively small. Coefficient of variation for posterior parameters estimates of the nonlinear oil dampers are then listed in Table 5, which can reflect the dispersion degree of the parameter posterior distribution. As can be observed from Table 5, the coefficient of variation for all parameters are within acceptable range. Among them, for the longitudinal direction (EW), the posterior distribution for parameter, k_{d1}, k_{d2} , both have the better accuracy with the smaller coefficient of variation value of 0.4% and 0.79%, respectively. While the viscous damping coefficient c_{d1} and c_{d2} show relatively large coefficient of variation, and the corresponding velocity exponent, α_{d1} and α_{d2} , possess the moderate coefficient of variation. On the contrary, for the transverse direction (NS), the parameter posterior distribution is multi-modal, and two obvious peaks can be observed for the uncertain parameters.

From the identified posterior parameter distribution depicted in Fig. 10, each parameter is basically independent with each other, except that the viscous damping coefficient c_{d1} and corresponding velocity exponent α_{d1} , whose joint posterior distribution indicates a linear correlation between themselves. Similarly, the viscous damping coefficient c_{d2} shows to be slightly linearly correlated with corresponding velocity exponent α_{d2} in Fig. 10. As can be observed from parameter posterior distribution illustrated in Fig. 11, the posterior distributions of any two parameters indicate to be a multi-modal distribution. In particular, the correlation between velocity exponent α_{d2} and other parameters looks like a step function. The identification results indicate that the proposed PF-MCMC approach can be successfully applied to non-Gaussian, high dimensional, even highly nonlinear and multi-modal system. Besides, in the process of the proposed PF-MCMC approach, the sampled particles propagate well without stuck to one or two special particles, which demonstrates that the proposed PF-MCMC approach is able to efficiently circumvent the problem of classical particle filtering methods. In the end, the model parameters, $k_{d1}, k_{d2}, c_{d1}, c_{d2}, \alpha_{d1}, \alpha_{d2}$, are estimated using the maximum a posteriori (MAP), and the MAP values of the parameter posterior distribution are illustrated in Table 6 for the nonlinear oil dampers in both directions.

The estimated damper force responses are then compared with their corresponding measurements of the nonlinear oil damper II as illustrated in Fig. 12, and the comparison of hysteresis loops for the nonlinear oil damper II are also depicted in Fig. 12. Normalized

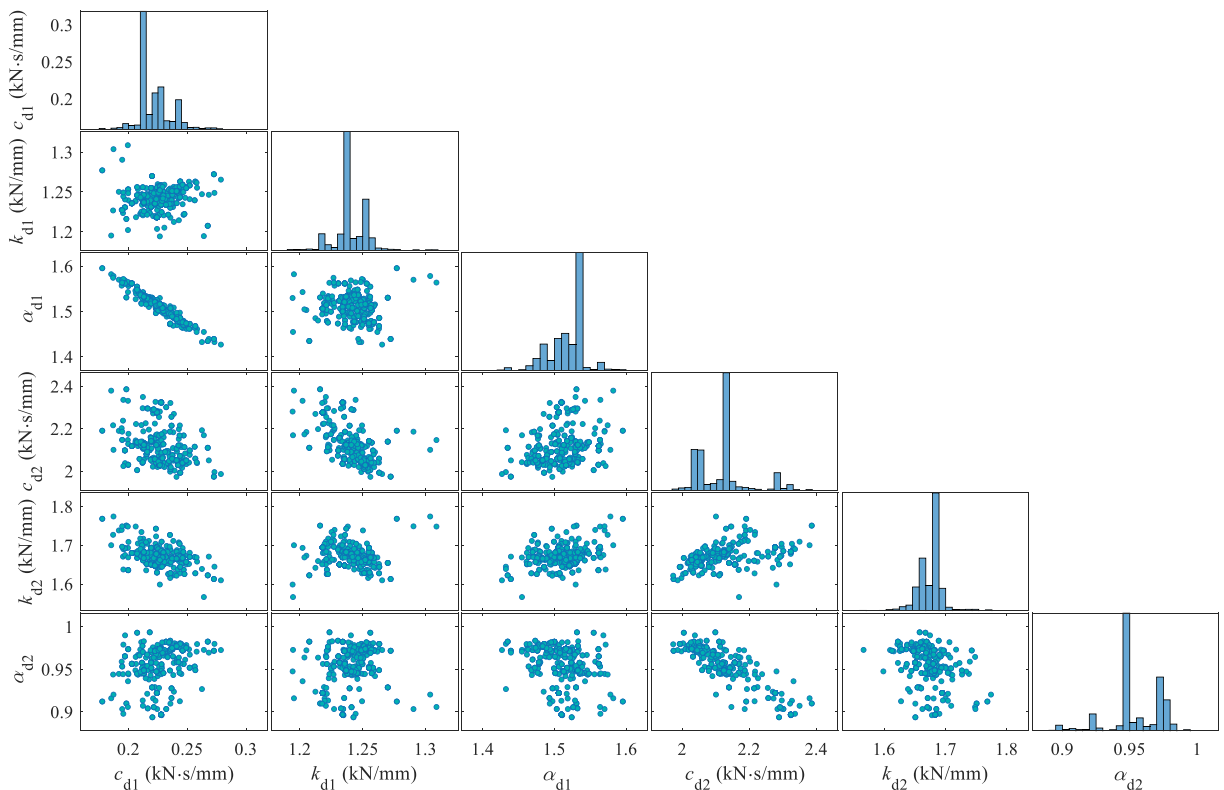


Fig. 10. Posterior distribution of identified parameters of complex model for nonlinear oil damper in longitudinal direction (EW).

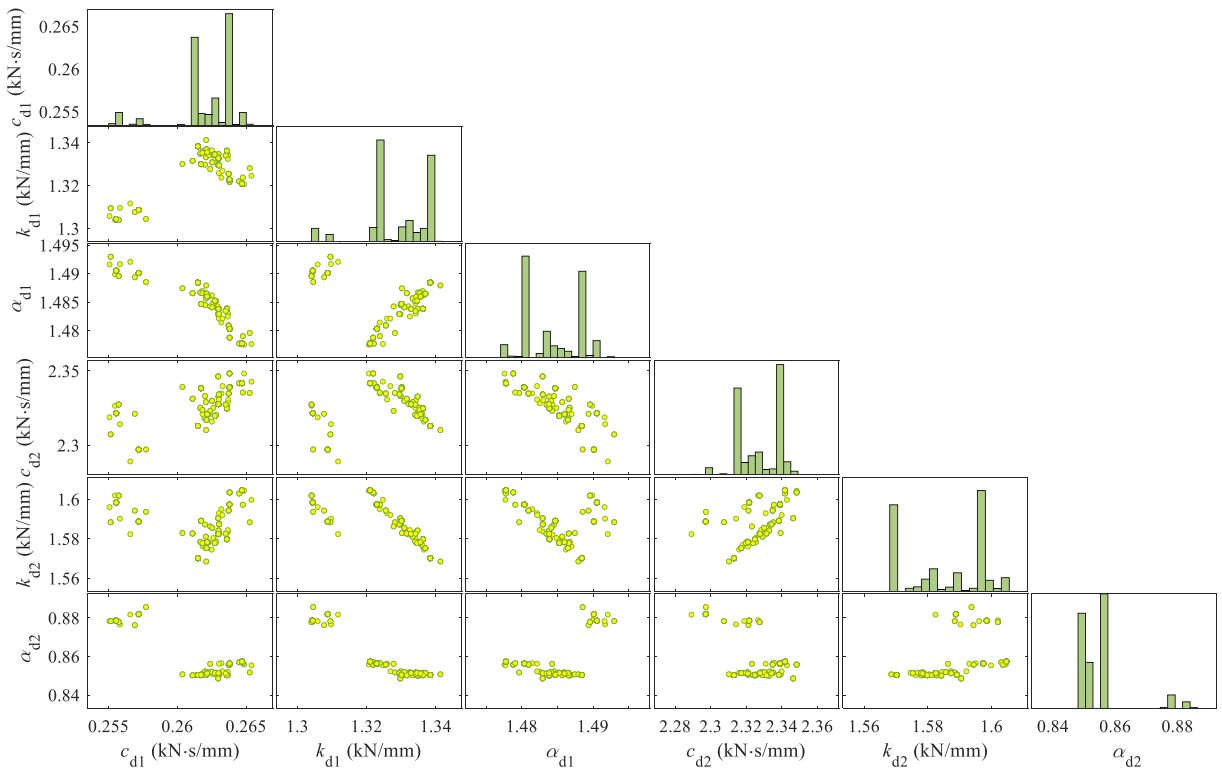


Fig. 11. Posterior distribution of identified parameters of complex model for nonlinear oil damper in transverse direction (NS).

Table 5
Coefficient of variation for posterior parameters estimates of the nonlinear oil dampers.

Damper type	Coefficient of variation	Direction	c_{d1}	k_{d1}	α_{d1}	c_{d2}	k_{d2}	α_{d2}
Damper II	δ	EW	0.0368	0.0040	0.0106	0.0121	0.0079	0.0063
		NS	0.0080	0.0070	0.0027	0.0054	0.0078	0.0089

root mean squared error (NRMS) is utilized to measure the accuracy for the estimated or predicted response, which can be defined as follows:

$$NRMS = \frac{\|F_d(t) - \hat{F}_d(t)\|}{\|F_d(t) - \text{mean}(F_d(t))\|} \tag{35}$$

where $\|\bullet\|$ represents the 2-norm function of a vector. $F_d(t)$ denotes the measured observation vector, $\hat{F}_d(t)$ is the corresponding posterior response estimates of the damper force. Here, the NRMS values vary between $-\text{Inf}$ and 1, and the NRMS value approximate to 0 indicates perfect fit with nearly zero error, the other way around represents bad fit.

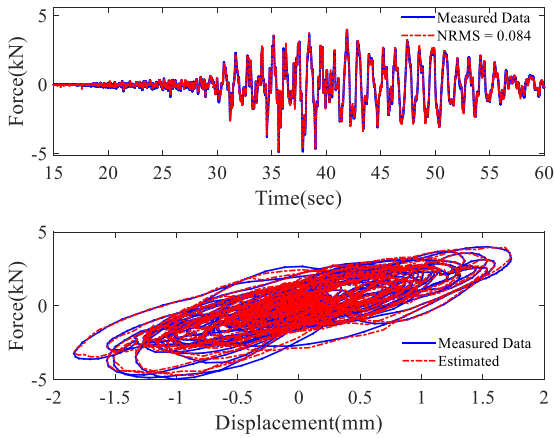
As can be seen in Fig. 12, the estimated damper force responses are well agreement with the corresponding measurements, and their NRMS values equal to 8.4% and 7.3% for longitudinal (EW) and transverse (NS) directions, respectively. Besides, the estimated hysteretic loops of the relative displacement versus the damper forces are also consistent with that of the recorded inter-story displacement versus the measured damper forces. The good consistency demonstrates that both states and parameters can be effectively identified by the proposed PF-MCMC approach.

To further validate the identified model and predict the model response of the nonlinear oil damper braces under other earthquakes, the recorded seismic response on 2005/08/16 is exploited to validate the training models which are defined by the posterior parameters identified under May 26th 2003 earthquake records. As it's often the case that identifying under different excitation signals yields different interpretations of the model, the final identified models are then evaluated by predicting the response of the nonlinear oil damper under the seismic recordings listed in Table 1. The comparison between the measured and predicted responses in longitudinal (EW) direction are then illustrated as an example in Fig. 13 and Fig. 14.

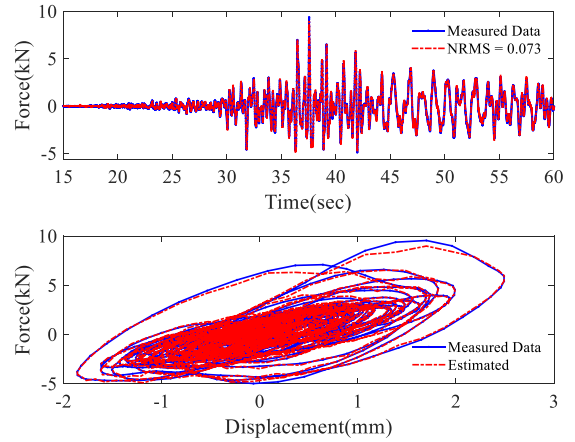
From the comparison results in Fig. 13, the NRMS values for seismic records, 2005/08/16, 2011/03/09 and 2011/04/07, are 23%, 31.1% and 18.6%, respectively. Noteworthy that the identified model is capable of more accurately replicating the dynamic behavior of the nonlinear oil damper under seismic record 2011/04/07 than 2011/03/09, which is partially because the responses of seismic

Table 6
MAP estimates of model parameters for nonlinear oil dampers.

Damper type	Direction	c_{d1} (kN•s/mm)	k_{d1} (kN /mm)	α_{d1}	c_{d2} (kN•s/mm)	k_{d2} (kN /mm)	α_{d2}
Damper II	EW	0.2702	1.2626	1.4507	1.9803	1.6172	0.9783
	NS	0.2630	1.3259	1.4821	2.3308	1.5930	0.8563

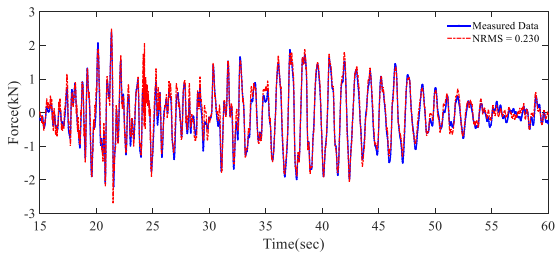


(a) Damper force and hysteretic loops comparison between identified and measured data (EW)

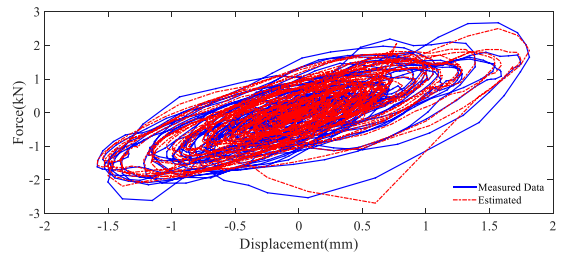


(b) Damper force and hysteretic loops comparison between identified and measured data (NS)

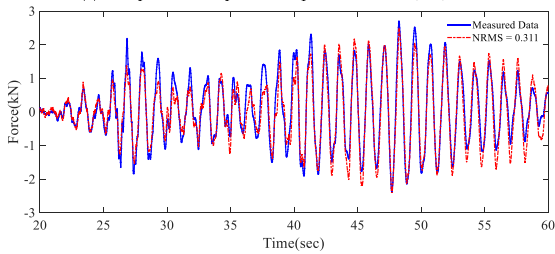
Fig. 12. Identification results for the nonlinear oil damper Type II on 8th floor in both longitudinal (EW) and transverse (NS) directions.



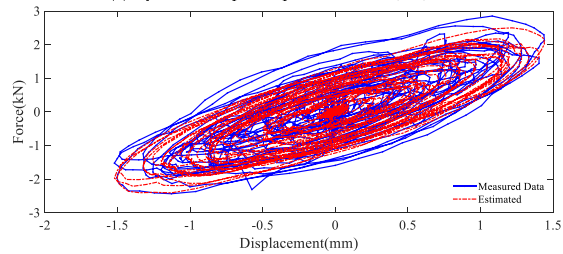
(a) Damper force response comparison for 2005/08/16



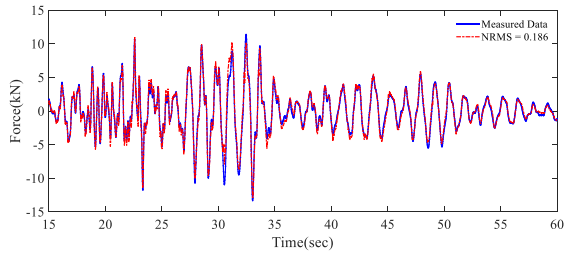
(b) Hysteretic loops comparison for 2005/08/16



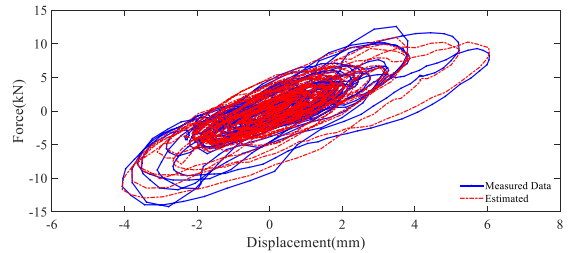
(c) Damper force comparison for 2011/03/09



(d) Hysteretic loops comparison for 2011/03/09



(e) Damper force response comparison for 2011/04/07



(f) Hysteretic loops comparison for 2011/04/07

Fig. 13. Model validation and prediction of the nonlinear oil damper Type II under strong earthquake records in longitudinal (EW) direction.

record 2011/04/07 are at a similar level of information with that of the identified model response. Besides, the displacement of the nonlinear oil damper is not necessary starting from zero, since the starting point is the same place where the last movement of the nonlinear oil damper stopped, which may incur a bias to the recorded data, as can be observed for record 2011/03/09. After all, the results of comparison between the measured and predicted responses clearly show that the identified model is able to capture main behavior of the nonlinear oil damper, and the complex model can be further used for model updating and prediction under future excitation of different spectral characteristics.

5. Conclusions

In this study, the analysis of a proposed new type oil damper with viscoelastic polymer packing soft rings is conducted. The proposed nonlinear oil damper is not only capable of avoiding precision machining of incorporating shaft bearings and pressure sealings, but also able to efficiently acquire vibration control effectivity with a small damper force. The nonlinear oil dampers are then applied to an eight-story passively-controlled steel building. Both structural health monitoring system and vibration monitoring instruments are installed for the building and nonlinear oil dampers, respectively. Based on the accumulated seismic response records of the nonlinear oil damper, the most probable model class which is capable of representing the dynamic behavior of the nonlinear oil damper is then picked using Bayesian model selection method among three candidate model classes. In the procedure of Bayesian model selection, selecting a model class merely according to the data-fit term in equation (7) may bring about over-fitting problem of the data which may result in poor subsequent response predictions or even be unreliable by the selected model class due to taking too much detail information from the specific data. Besides, more complex models prefer over simpler models based on the data-fit term. While the Ockham’s razor prefers to simpler models over more complex models, if the simpler models produce reasonably consistency with the data, and just slightly worse than the complex models. Finally, a trade-off between the information-theoretic complexity and data-fit of the model class is established with a penalty against complex models for Bayesian model selection method.

To further investigate actual performance and dynamic characteristics of the nonlinear oil damper, reliable model identification methods are necessary to estimate the model of the nonlinear oil dampers. The classical particle filtering algorithm is developed to identify parameter of the nonlinear model and quantify the model uncertainties at the same time. The developed particle filter is capable of re-parameterizing joint posterior distribution of states and parameters of the nonlinear oil damper without augmented state estimation, which combined with Markov chain Monte Carlo algorithm so as to be able to sample high-dimensional posterior distribution. The identification results indicate that the proposed PF-MCMC approach can be successfully applied to non-Gaussian, high

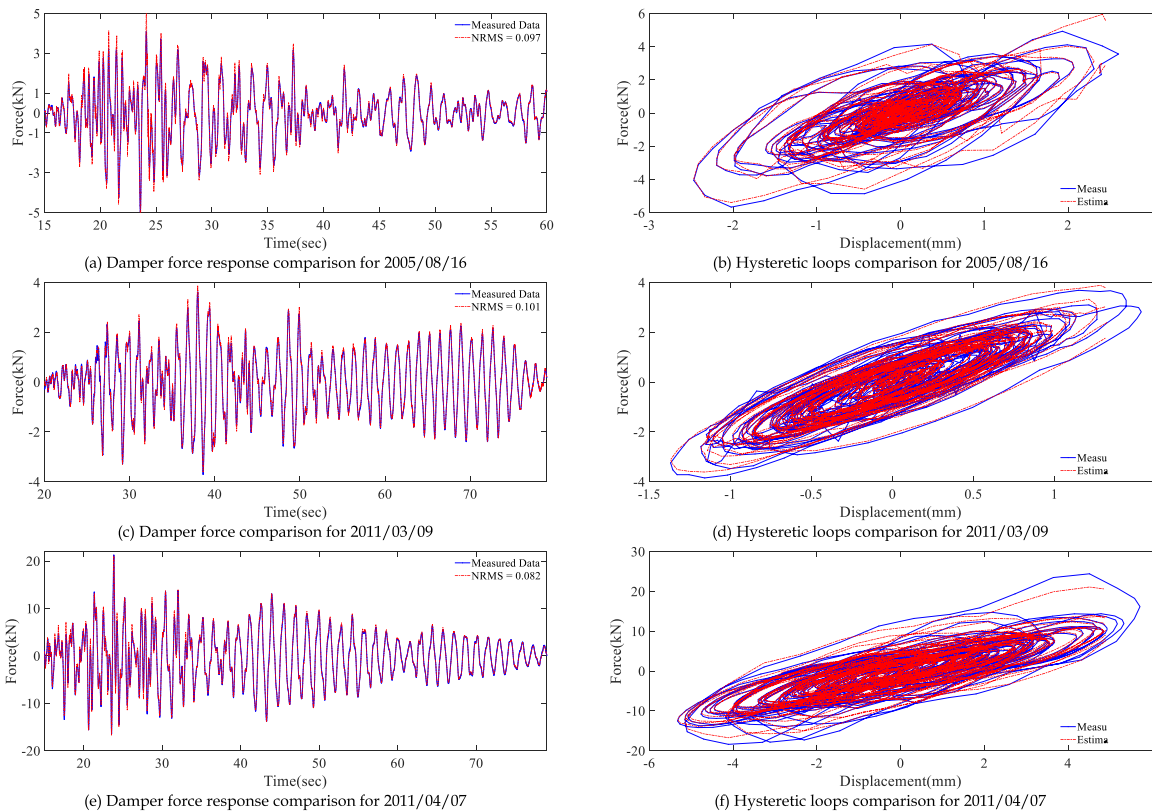


Fig. 14. Model validation and prediction of the nonlinear oil damper Type II under strong earthquake records in transverse (NS) direction.

dimensional, even highly nonlinear and multi-modal system. Besides, in the procedure of the proposed PF-MCMC approach, the samples propagate well without stuck to special particles, which demonstrates that the proposed PF-MCMC approach can efficiently circumvent the problem of classical particle filtering methods.

The estimated models are then validated and evaluated with respect to the recorded seismic response for 2005/08/16, 2011/03/09 and 2011/04/07, and the final identified model is then evaluated by predicting the response of the nonlinear oil damper. From the results of comparison between the measured and predicted responses, it's clearly shown that the identified model is able to capture main behavior of the nonlinear oil damper. Furthermore, the complex model can be incorporated into structural models for model updating and prediction in whole based on the vibration data of structural health monitoring system, as well as for design optimization.

Declaration of Competing Interest

The authors declare that they have no known competing financial interests or personal relationships that could have appeared to influence the work reported in this paper.

Data availability

Data will be made available on request.

Acknowledgements

The authors express their sincere thanks to the research team who conducted the structural health monitoring of a passively controlled eight-story steel building with various types of dampers (Leader: Professor Songtao Xue, Tongji University and Tohoku Institute of Technology). The authors also acknowledge the financial support from Funds National Natural Science Foundation of China (Grant No. 2021YFE0112200), the Natural Science Foundation of Shanghai (Grant No. 20ZR1461800), and the Tohoku Institute of Technology research Grant. The findings in this paper are those of the authors and do not necessary reflect the view of the sponsors.

References

- [1] H. Sarmadi, K. Yuen, Structural health monitoring by a novel probabilistic machine learning method based on extreme value theory and mixture quantile modeling, *Mech. Syst. Signal Process.* 173 (2022), 109049.
- [2] M.P. Singh, N.P. Verma, L.M. Moreschi, Seismic analysis and design with Maxwell dampers, *J. Eng. Mech.* 129 (3) (2003) 273–282.
- [3] Y. Liu, J. Wu, M. Donà, Effectiveness of fluid-viscous dampers for improved seismic performance of inter-storey isolated buildings, *Eng. Struct.* 169 (2018) 276–292.
- [4] A. Ras, N. Boumechra, Seismic energy dissipation study of linear fluid viscous dampers in steel structure design, *Alex. Eng. J.* 55 (3) (2016) 2821–2832.
- [5] M.C. Constantinou, M.D. Symans, Experimental and analytical investigation of seismic response of structures with supplemental fluid viscous dampers, National Center for earthquake engineering research Buffalo, NY, 1992.
- [6] G.K. Hüffmann, Full base isolation for earthquake protection by helical springs and viscodampers, *Nucl. Eng. Des.* 84 (3) (1985) 331–338.
- [7] Constantinou, M.C., T.T. Soong and G.F. Dargush, Passive energy dissipation systems for structural design and retrofit. 1998.
- [8] M.C. Constantinou, M.D. Symans, Experimental study of seismic response of buildings with supplemental fluid dampers, *Struct. Des. Tall Build.* 2 (2) (1993) 93–132.
- [9] N. Makris, G.F. Dargush, M.C. Constantinou, Dynamic analysis of generalized viscoelastic fluids, *J. Eng. Mech.* 119 (8) (1993) 1663–1679.
- [10] N. Makris, M.C. Constantinou, Fractional-derivative Maxwell model for viscous dampers, *J. Struct. Eng.* 117 (9) (1991) 2708–2724.
- [11] C.G. Koh, J.M. Kelly, Application of fractional derivatives to seismic analysis of base-isolated models, *Earthq. Eng. Struct. Dyn.* 19 (2) (1990) 229–241.
- [12] N. Makris, M.C. Constantinou, A.M. Reinhorn, Viscous dampers: testing, modeling and application in vibration and seismic isolation, National Center for Earthquake Engineering Research, Buffalo, NY, USA, 1990.
- [13] X. Hu, C. Zhou, The effect of various damping on the isolation performance of quasi-zero-stiffness system, *Mech. Syst. Sig. Process.* 171 (2022), 108944.
- [14] A.Q. Bhatti, H. Varum. Comparison between the visco-elastic dampers and magnetorheological dampers and study the effect of temperature on the damping properties. 2012.
- [15] A. Rodriguez, et al., Model identification of a large-scale magnetorheological fluid damper, *Smart Mater. Struct.* 18 (1) (2008), 015010.
- [16] K. Oohara, K. Kasai. Time-history analysis model for nonlinear viscous dampers. 2002.
- [17] W. Lin, A.K. Chopra, Earthquake response of elastic SDF systems with non-linear fluid viscous dampers, *Earthq. Eng. Struct. Dyn.* 31 (9) (2002) 1623–1642.
- [18] G. Terenzi, Dynamics of SDOF systems with nonlinear viscous damping, *J. Eng. Mech.* 125 (8) (1999) 956–963.
- [19] A.A. Seleemah, M.C. Constantinou, Investigation of seismic response of buildings with linear and nonlinear fluid viscous dampers, National Center for Earthquake Engineering Research Buffalo, 1997.
- [20] A.M. Reinhorn, C. Li and M.C. Constantinou, Experimental and analytical investigation of seismic retrofit of structures with supplemental damping: Part. 1-fluid viscous damping devices. 1995. p. 120-120.
- [21] X. Ji, et al., Damping identification of a full-scale passively controlled five-story steel building structure, *Earthq. Eng. Struct. Dyn.* 42 (2) (2013) 277–295.
- [22] F. Adachi, et al., Nonlinear optimal oil damper design in seismically controlled multi-story building frame, *Soil Dyn. Earthq. Eng.* 44 (2013) 1–13.
- [23] H. Kurino et al., Switching oil damper with built-in controller for structural control. *Journal of structural engineering* (New York, N.Y.), 2003. 129(7): p. 895-904.
- [24] K. Kasai, K. Matsuda, Full-scale dynamic testing of response-controlled buildings and their components: concepts, methods, and findings, *Earthq. Eng. Eng. Vib.* 13 (S1) (2014) 167–181.
- [25] S. Matsuda, Optimum design of Maxwell-type damper system based on stochastically equivalent damping factor. 2012.
- [26] K. Kasai, et al., Full-scale tests of passively-controlled 5-story steel building using E-Defense shake table Part 1: Test concept, method, and building specimen: K. Kasai & S. Motoyui H. Ozaki & M. Ishii. 2009, CRC Press. p. 29-36.
- [27] O. Takahashi, Y. Sekiguchi. Constitutive rule of oil damper with Maxwell model and source code for analysis program. 2001.
- [28] S. Kawamata, N. Funaki and Y. Itoh. Passive control of building frames by means of liquid dampers sealed by viscoelastic material. in: 12th World Conference on Earthquake Engineering. 2000.
- [29] Y.T. Chen, Y.H. Chai, Effects of brace stiffness on performance of structures with supplemental Maxwell model-based brace-damper systems, *Earthq. Eng. Struct. Dyn.* 40 (1) (2011) 75–92.
- [30] Y.T. Chen, Y.H. Chai. Seismic design of structures with supplemental Maxwell model-based brace-damper systems. 2008.

- [31] N. Funaki, J. Kang and S. Kawamata, Vibration response of a three-storied full-scale test building passively controlled by liquid dampers sealed by viscoelastic material. 2001.
- [32] M. Witters, J. Swevers, Black-box model identification for a continuously variable, electro-hydraulic semi-active damper, *Mech. Syst. Sig. Process.* 24 (1) (2010) 4–18.
- [33] S.M. Savaresi, S. Bittanti, M. Montiglio, Identification of semi-physical and black-box non-linear models: the case of MR-dampers for vehicles control, *Automatica* 41 (1) (2005) 113–127.
- [34] K. Worden, et al., Nonlinear system identification of automotive dampers: A time and frequency-domain analysis, *Mech. Syst. Sig. Process.* 23 (1) (2009) 104–126.
- [35] Y.A. Yucesan, et al., Adjusting a torsional vibration damper model with physics-informed neural networks, *Mech. Syst. Sig. Process.* 154 (2021), 107552.
- [36] S. Wei, J. Wang, J. Ou, Method for improving the neural network model of the magnetorheological damper, *Mech. Syst. Sig. Process.* 149 (2021), 107316.
- [37] H. Metered, P. Bonello, S.O. Oyadiji, The experimental identification of magnetorheological dampers and evaluation of their controllers, *Mech. Syst. Sig. Process.* 24 (4) (2010) 976–994.
- [38] M. Zapateiro, et al., Vibration control of a class of semiactive suspension system using neural network and backstepping techniques, *Mech. Syst. Sig. Process.* 23 (6) (2009) 1946–1953.
- [39] G. Quaranta, G. Monti, G.C. Marano, Parameters identification of Van der Pol-Duffing oscillators via particle swarm optimization and differential evolution, *Mech. Syst. Sig. Process.* 24 (7) (2010) 2076–2095.
- [40] E.N. Chatzi, A.W. Smyth, The unscented Kalman filter and particle filter methods for nonlinear structural system identification with non-collocated heterogeneous sensing, *Struct. Control Health Monit.* 16 (1) (2009) 99–123.
- [41] S. Akcelyan, D.G. Lignos, T. Hikino, Adaptive numerical method algorithms for nonlinear viscous and bilinear oil damper models subjected to dynamic loading, *Soil Dyn. Earthq. Eng.* 113 (2018) 488–502.
- [42] I. López, J.M. Busturia, H. Nijmeijer, Energy dissipation of a friction damper, *J. Sound Vib.* 278 (3) (2004) 539–561.
- [43] M. Cao, et al., Performance Study of an 8-story Steel Building Equipped with Oil Damper Damaged During the 2011 Great East Japan Earthquake Part 2: Novel Retrofit Strategy, *J. Asian Architect. Build. Eng.* 15 (2) (2018) 303–310.
- [44] J.L. Beck, K. Yuen, Model selection using response measurements: Bayesian probabilistic approach, *J. Eng. Mech.* 130 (2) (2004) 192–203.
- [45] D.J.C. Mackay, *Bayesian methods for adaptive models.* 1992, California Institute of Technology.
- [46] J. Ching, M. Muto and J.L. Beck. *Bayesian linear structural model updating using Gibbs sampler with modal data.* 2005: Millpress.
- [47] E.T. Jaynes, *Probability theory: The logic of science.* 2003: Cambridge university press.
- [48] S. Särkkä, *Bayesian filtering and smoothing.* 2013: Cambridge University Press.
- [49] Haug, A.J., *Bayesian estimation and tracking: a practical guide.* 2012: John Wiley & Sons.
- [50] J.S. Liu, R. Chen, Sequential Monte Carlo methods for dynamic systems, *J. Am. Stat. Assoc.* 93 (443) (1998) 1032–1044.
- [51] J. Liu, M. West, in: Combined parameter and state estimation in simulation-based filtering, Springer, 2001, pp. 197–223.
- [52] T.C. Clapp, *Statistical methods for the processing of communications data,* University of Cambridge, 2001.
- [53] O. Cappé, S.J. Godsill, E. Moulines, An overview of existing methods and recent advances in sequential Monte Carlo, *Proc. IEEE* 95 (5) (2007) 899–924.
- [54] N. Gordon, *Beyond the Kalman filter: Particle filters for tracking applications.* 2004.
- [55] F.E. Daum, J. Huang, Dynamic quasi-Monte Carlo for nonlinear filters, *Int. Soc. Optics Photonics* (2003).
- [56] B. Ristic, S. Arulampalam, N. Gordon, *Beyond the Kalman filter: Particle filters for tracking applications,* Artech house, 2003.
- [57] C. Andrieu, A. Doucet, Particle filtering for partially observed Gaussian state space models, *J. R. Statist. Soc. Series B Statist. Methodol.* 64 (4) (2002) 827–836.
- [58] K. Erazo, S. Nagarajaiah, An offline approach for output-only Bayesian identification of stochastic nonlinear systems using unscented Kalman filtering, *J. Sound Vib.* 397 (2017) 222–240.
- [59] M. Khalil, et al., The estimation of time-invariant parameters of noisy nonlinear oscillatory systems, *J. Sound Vib.* 344 (2015) 81–100.
- [60] C. Andrieu, A. Doucet, R. Holenstein, Particle Markov chain Monte Carlo methods, *J. R. Stat. Soc. Ser. B (Stat Methodol.)* 72 (3) (2010) 269–342.